

1 **Intact polar lipids in the water column of the Eastern Tropical North Pacific: Abundance and**
2 **structural variety of non-phosphorus lipids**

3 Florence Schubotz ^{1*}, Sitan Xie ^{1,¶}, Julius S. Lipp ¹, Kai-Uwe Hinrichs ¹, Stuart G. Wakeham ²

4

5

6 ¹MARUM and Department of Geosciences, University of Bremen, 28359 Bremen, Germany

7 ²Skidaway Institute of Oceanography, Savannah, GA 31411, USA

8 [¶]Current address: Wai Gao Qiao Free Trade Zone, 200131 Shanghai, China

9

10

11

12

13

14

15

16

17 ^{*}Corresponding author. MARUM, University of Bremen, Leobener Str. 13, Room 1070, 28359 Bremen,
18 Germany. Tel: +49-421-218-65724. Fax: +49-421-218-65715. E-mail: schubotz@uni-bremen.de

19

20 **Keywords:** intact polar lipids, phospholipids, glycolipids, betaine lipids, ether lipids, oxylipins,
21 phospholipid substitution, oxygen minimum zone

22 **Abstract**

23 Intact polar lipids (IPLs) are the main building blocks of cellular membranes and contain
24 chemotaxonomic, ecophysiological and metabolic information, making them valuable biomarkers in
25 microbial ecology and biogeochemistry. This study investigates IPLs in suspended particulate matter
26 (SPM) in the water column of the Eastern Tropical North Pacific Ocean (ETNP), one of the most extensive
27 open ocean oxygen minimum zones (OMZ) in the world with strong gradients of nutrients, temperature
28 and redox conditions. A wide structural variety in polar lipid head group composition and core structures
29 exists along physical and geochemical gradients within the water column, from the oxygenated photic
30 zone to the aphotic OMZ. We use this structural diversity in IPLs to evaluate the ecology and
31 ecophysiological adaptations that affect organisms inhabiting the water column, especially the mid-depth
32 OMZ in the context of biogeochemical cycles. Diacylglycerol phospholipids are present at all depths,
33 but exhibit highest relative abundance and compositional variety (including mixed acyl/ether core
34 structures) in the upper and core OMZ where prokaryotic biomass was enriched. Surface ocean SPM is
35 dominated by diacylglycerol glycolipids that are found in photosynthetic membranes. These and other
36 glycolipids with varying core structures composed of ceramides and hydroxylated fatty acids are also
37 detected with varying relative abundances in the OMZ and deep oxycline, signifying additional non-
38 phototrophic bacterial sources for these lipids. Betaine lipids (with zero or multiple hydroxylations in
39 the core structures) that are typically assigned to microalgae are found throughout the water column down
40 to the deep oxycline but do not show a depth-related trend in relative abundance. Archaeal IPLs
41 comprised of glycosidic and mixed glycosidic-phosphatidic glycerol dibiphytanyl glycerol tetraethers
42 (GDGTs) are most abundant in the upper OMZ where nitrate maxima point to ammonium oxidation, but

43 increase in relative abundance in the core OMZ and deep oxycline. The presence of non-phosphorus
44 “substitute” lipids within the OMZ suggest that the indigenous microbes might be phosphorus limited (P
45 starved) at ambient phosphate concentrations of 1 to 3.5 μM , although specific microbial sources for many
46 of these lipids still remain unknown.

47 **1. Introduction**

48 Oxygen Minimum Zones (OMZ) are permanently oxygen-deficient regions in the ocean defined by
49 O₂ concentrations <20 μM. They occur in areas where coastal or open ocean upwelling of cold, nutrient-
50 rich waters drive elevated levels of primary production and the subsequent respiration of organic matter
51 exported out of productive surface waters consumes oxygen faster than it is replaced by ventilation or by
52 mid-depth lateral injections of oxygenated water. Low oxygen levels cause habitat compression,
53 whereby species intolerant to low levels of oxygen are restricted to oxygenated surface waters (Keeling
54 et al., 2010; Rush et al., 2012). But even these low levels of oxygen permit vertical migration of some
55 zooplankton taxa into hypoxic waters (e.g., Seibel, 2011; Wishner et al., 2013). Oxygen depletion
56 stimulates diverse microbial life capable of utilizing alternative electron acceptors for respiration under
57 microaerobic conditions (e.g., Ulloa et al., 2012; Tiano et al., 2014; Carolan et al., 2015; Kalvelage et al.,
58 2015; Duret et al., 2015). Important prokaryote-mediated processes within OMZs include denitrification
59 and the anaerobic oxidation of ammonium (anammox), which together may account for 30-50% of the
60 total nitrogen loss from the ocean to the atmosphere (Gruber, 2008; Lam and Kuypers, 2011). Modern
61 day OMZs comprise ~8% of global ocean volume (Karstensen et al., 2008; Paulmier and Ruiz-Pino, 2009;
62 Lam and Kuypers, 2011), but any expansion in the coming decades as a consequence of global warming
63 and increased stratification (Stramma et al., 2008; Keeling et al., 2010) would have profound effects on
64 marine ecology, oceanic productivity, global carbon and nitrogen cycles, the biological pump and
65 sequestration of carbon (Karstensen et al., 2008; Stramma et al., 2010; Wright et al., 2012). A better
66 understanding of the effect of low-O₂ on marine biogeochemistry and microbial ecology is thus warranted.

67 The Eastern Tropical North Pacific Ocean (ETNP), situated off the west coast of Mexico and Central
68 America, hosts one of the largest OMZs in the open ocean, extending halfway across the Pacific Ocean
69 and comprising ~41% of global OMZs (Lavin and Fiedler, 2006; Fiedler and Talley, 2006; Paulmier and
70 Ruiz-Pino, 2009). By comparison, OMZs of the Eastern Tropical South Pacific Ocean off Peru and Chile
71 and in the Arabian Sea are ~14% and ~8%, respectively, of global OMZs. In the ETNP, a sharp
72 permanent pycnocline develops where warm, saline surface waters lie on top of a shallow thermocline,
73 producing a highly stratified water column. Moderate primary production, dominated by picoplankton,
74 depends on oceanic upwelling and wind mixing of coastal waters but is generally limited by the lack of
75 micronutrient dissolved iron (Franck et al., 2005; Pennington et al., 2006). Remineralization, ~70% of
76 which is microbially mediated (Cavan et al., 2017), of particulate organic carbon exported out of surface
77 waters consumes oxygen at rates that cannot be balanced by ventilation across the pycnocline and by
78 sluggish lateral circulation, leading to O₂ levels <2 μM at depths between ~100 and ~800 m.
79 Abundances of micro- (Olson and Daly, 2013) and macro-zooplankton (Wishner et al., 2013; Williams et
80 al., 2014) that are high in surface waters are reduced in the OMZ, and those macrozooplankton that are
81 diel vertical migrators survive in the OMZ with reduced metabolic rates (Maas et al., 2014; Cass and Daly,
82 2015). Microbial abundances and activities for both heterotrophic and chemoautotrophic metabolisms
83 are high in both surface waters and within the OMZ, but again with reduced metabolic rates in the OMZ
84 (Podlaska et al., 2012). A strong nutricline indicates microbial nitrogen cycling involving co-occurring
85 nitrification, denitrification and anammox (Rush et al., 2012; Podlaska et al., 2012), perhaps contributing
86 up to 45% of the global pelagic denitrification (Codispoti and Richards, 1976). Microbial communities
87 are mainly comprised of proteobacteria, with increasing contributions of archaea in deeper waters. Yet, on

88 average ca. 50% of the prokaryotic communities within the OMZ of the ETNP remained uncharacterized
89 (Podlaska et al., 2012).

90 Intact polar lipids (IPLs) are the main building blocks of cellular membranes and may be used to
91 characterize abundance and physiology of aquatic microorganisms from all three domains of life. IPLs
92 represent a diverse range of molecular structures, including phosphatidyl, glycosidic, phospho-glycosidic,
93 and amino acid polar head groups linked to glyceryl-acyl and glyceryl-*O*-alkyl apolar moieties. IPL
94 distributions have been documented in surface waters of the Eastern Subtropical South Pacific (Van Mooy
95 and Fredricks, 2010), the Western North Atlantic Ocean (Van Mooy et al., 2006; 200; Pependorf et al.,
96 2011a), the South Pacific Ocean (Kharbush et al., 2016), the Mediterranean Sea (Pependorf, et al., 2011b),
97 the North Sea (Brandsma et al., 2012), lakes (Bale et al., 2016), the Western English Channel (White et
98 al., 2015) and throughout the water columns of stratified water bodies (Ertefai et al., 2008; Schubotz et
99 al., 2009; Wakeham et al., 2012; Pitcher et al., 2011; Xie et l., 2014; Basse et al., 2014; Sollai et al., 2015).
100 Surface waters are typically dominated by nine IPL classes. Three diacylglycerol glycolipids,
101 monoglycosyl (1G-), diglycosyl (2G-) and sulfoquinovosyl diacylglycerol (SQ-DAG), are main IPLs
102 found in all thylakoid membranes of phototrophs, including those of cyanobacteria (Siegenthaler et al.,
103 1998)¹. Three betaine lipids, diacylglyceryl homoserine (DGTS), hydroxymethyl-trimethyl- β -alanine
104 (DGTA) and carboxy-*N*-hydroxymethyl-choline (DGCC), are also generally abundant. Betaine lipids
105 are widely distributed in lower plants and green algae (Dembitsky, 1996) and are thus usually assigned to

¹ Elsewhere in the literature 1G-DAG, 2G-DAG, and SQ-DAG are also termed MGDG, DGDG and SQDG. However, we have opted to retain the 1G-DAG, 2-DAG, etc. nomenclature as other IPLs discussed throughout also contain monoglycosyl- and diglycosyl-moieties (e.g., 1G-GDGT and 2G-GDGT). Likewise, we retain the nomenclature PC-DAG, PE-DAG, and PG-DAG for phospholipids elsewhere termed PC, PE, PG.

106 eukaryotic algae in the ocean (Popendorf, et al., 2011a), but DGTS was recently also found in bacteria
107 when phosphorus is limited (Yao et al., 2015; Sebastian et al. 2016). Three common detected
108 phospholipids are diacylglycerol phosphatidyl choline (PC-DAG; often simply referred to elsewhere as
109 PC), phosphatidyl ethanolamine (PE-DAG, often PE), and phosphatidyl glycerol (PG-DAG, often PG),
110 all of which have mixed eukaryotic or bacterial sources in the upper water column (Sohlenkamp et al.,
111 2003; Popendorf, et al., 2011a). Microbial source assignments have been broadly confirmed by isotope
112 labeling studies (Popendorf, et al., 2011a). In oxygen-deficient subsurface waters IPL distributions are
113 more diverse and other phospholipids such as diacylglycerol phosphatidyl (*N*)-methylethanolamine
114 (PME-DAG), phosphatidyl (*N,N*)-dimethylethanolamine (PDME-DAG) and diphosphatidyl glycerol
115 (DPG) increase in abundance; these IPLs occur in a number of bacteria that may inhabit low oxygen
116 environments (Schubotz et al., 2009; Wakeham et al., 2012). Dietherglycerol phospholipids and
117 glycosidic ceramides with unidentified sources have also been detected (Schubotz et al., 2009; Wakeham
118 et al., 2012), the latter have been recently observed to be abundant in phosphorus-limited diatoms (Hunter
119 et al., 2018). IPLs that are unique to marine archaea are comprised of glycerol dialkyl glycerol tetraethers
120 (GDGT) core lipids with various glycosidic, diglycosidic and mixed phospho-glyco polar head groups
121 (e.g., Schouten et al., 2008; Pitcher et al., 2011; Zhu et al., 2016; Elling et al., 2017). Abundances of
122 archaeal IP-GDGTs vary considerably with depth, but are typically elevated in zones of water column
123 oxygen depletion, especially where ammonium oxidizing thaumarchaea are abundant (Pitcher et al., 2011;
124 Schouten et al., 2012; Sollai et al., 2015).

125 IPL can also be indicators of metabolic and physiologic status. Many organisms remodel their IPL
126 composition when faced with environmental stressors such as changes in pH, salinity, temperature or

127 availability of nutrients (Zhang and Rock, 2008; Van Mooy et al., 2009; Meador et al., 2014; Carini et al.,
128 2015; Elling et al., 2015). Replacing phospholipids with non-phosphorus containing substitute lipids is
129 an important mechanism when facing nutrient phosphate starvation in oligotrophic surface waters where
130 phosphate concentrations may be as low as nanomolar levels. Cyanobacteria replace PG-DAG with SQ-
131 DAG (Benning et al., 1993; Van Mooy et al., 2006) and microalgae and some bacteria replace PC-DAG
132 with DGTS (Geiger et al., 1999; Van Mooy et al., 2009; Pependorf, et al., 2011b) due to their similar ionic
133 charge at physiological pH. Heterotrophic marine bacteria can replace PE-DAG with either 1G-DAG or
134 DGTS (Carini et al., 2015; Sebastian et al., 2016; Yao et al., 2015). Notably, substitute lipids are also
135 biosynthesized under micromolar concentrations of phosphate (Bosak et al., 2016).

136 Here, we use IPL distributions in suspended particulate matter (SPM) to characterize eukaryotic,
137 bacterial and archaeal communities inhabiting the water column of the ETNP. This study is an extension
138 of that of Xie et al. (2014), which focused on the distribution of core and intact polar archaeal and bacterial
139 tetraether lipids at two stations investigated here (stations 1 and 8). The water column of the ETNP
140 comprises distinct biogeochemical zones based on oxygen concentrations and IPL distributions reflect the
141 localized ecology. Abundant non-phosphorus substitute lipids within the core of the OMZ suggest
142 phosphorus limitation of the source microorganisms even at micromolar concentrations of phosphate.
143 Overall our results provide deeper insight into the broad community composition and the physiologic state
144 of microorganisms inhabiting OMZs.

145

146 **2. Methods**

147 *2.1 Sample collection and CTD data*

148 Suspended particulate matter (SPM) samples were collected at four stations (distance to shore:
149 400~600 km; Fig 1) along a northwest-southeast transect (Station 1: 13° 01.87'N, 104° 99.83'W; Station
150 2: 11° 99.96' N, 101° 22.82' W; Station 5: 10° 68.94' N, 96° 34.12' W; and Station 8: 8° 99.46'N,
151 90°00.18'W) in the ETNP during the R/V *Seward Johnson* cruise in November 2007 (R/V *Seward Johnson*
152 Cruise Scientists, 2007). Station 1 in the Tehuantepec Bowl is an area of relatively low primary
153 productivity (e.g., 0.05 mg Chl-*a*/m²; (Fiedler and Talley, 2006; Pennington et al., 2006) whereas Station
154 8 in the Costa Rica Dome is moderately productive (1 mg Chl-*a*/m²). All stations are characterized by a
155 strong thermocline/pycnocline/oxycline (at 20-50 m depths depending on location) and a profound and
156 thick OMZ (down to ~2 μM O₂ between ~300-800 m depth). Station 1 is a reoccupation of the Vertical
157 Transport and Exchange II/III site from the early 1980's (Lee and Cronin, 1984; Martin et al., 1987;
158 Wakeham and Canuel, 1988; Wakeham, 1987, 1989).

159 Seawater was filtered *in-situ* using submersible pumps (McLane Research Laboratories WTS-142
160 filtration systems) deployed on the conducting cable of the CTD/rosette that measured temperature,
161 conductivity, oxygen, fluorescence/chlorophyll-*a* and transmissivity during pump deployments and
162 during pumping. Filtered water volumes ranged between 130 and 1800 L (Suppl. Table 1). Pumps
163 were fitted with two-tier 142 mm diameter filter holders: a 53 μm mesh Nitex “prefiltration” screen to
164 remove larger eukaryotes and marine snow aggregates and a double-stacked tier of ashed glass fiber filters
165 (142 mm Gelman type A/E, nominal pore size 0.7 μm). IPL concentrations we report represent minimum
166 values to reflect potentially inefficient collection of 0.7 μm particles by GFFs. Since pore size of the
167 filters may also decrease during filtration the recovered material may vary dependent on filtration time.

168 Following pump recovery, GFF filters and Nitex screens were wrapped in pre-combusted foil and stored
169 frozen at -20°C until extraction.

170

171 *2.2 Elemental, pigment and nutrient analysis*

172 Particulate organic carbon (POC) and total particulate nitrogen (TN) were measured on 14 mm-
173 diameter subsamples of each glass fiber filter (GFF) prior to lipid extraction; therefore, POC and TN
174 concentrations reported here are only for <53 µm material. The plugs were acidified in HCl vapor in a
175 desiccator for 12 hours to remove inorganic carbon. Elemental analysis was performed with a
176 ThermoFinnigan Flash EA Series 1112 interfaced to a ThermoFinnigan Delta V isotope ratio mass
177 spectrometer at the Skidaway Institute Scientific Stable Isotope Laboratory. Organic carbon and
178 nitrogen contents were calibrated against internal laboratory chitin powder standards which in turn had
179 previously been cross-calibrated against USGS 40 and 41 international standards.

180 Chlorophyll-*a* (Chl-*a*) and pheopigment concentrations were measured on-board the ship (Olson and
181 Daly, 2013). Seawater samples (100 – 500 ml) from CTD casts were filtered onto Whatman GF/F filters
182 (0.7 µm) which were immediately extracted with 90% acetone. Fluorescence was measured with a
183 Turner Designs 10AU fluorometer and Chl-*a* concentrations were determined after Parsons et al (1984).
184 Post-cruise HPLC analysis of pigments in 100 – 500 ml seawater samples filtered onto Whatman GF/F
185 (0.7 µm) filters were conducted at the College of Charleston Grice Marine Laboratory, Charleston, SC on
186 a Hewlett Packard 1050 system (DiTullio and Geesey, 2002).

187 Seawater samples for nutrient analyses (NO_2^- , NO_3^- , NH_4^+ and PO_4^{3-}) were collected directly from
188 Niskin bottles into acid-washed, 30-mL high-density polyethylene (HDP) bottles. After three rinses,

189 bottles were filled to the shoulder, sealed, and frozen (-20°C). All frozen samples were transported to
190 the Oceanic Nutrient Laboratory at USF for analysis using a Technicon Autoanalyzer II.

191

192 *2.3 Lipid extraction and analysis of intact polar lipids*

193 Lipids associated with the $<53\ \mu\text{m}$ SPM on the GFFs were Soxhlet-extracted shortly after the
194 expedition in 2008 using dichloromethane:methanol (DCM:MeOH; 9:1 v/v) for 8 h. Extracted lipids
195 were partitioned into DCM against 5% NaCl solution and dried over Na_2SO_4 . Total lipid extracts (TLEs)
196 were stored at -20°C . Soxhlet extractions, rather than for example microwave assisted Bligh-Dyer
197 extractions, were chosen at the time because it was the only feasible way to handle the double 142mm
198 filters. Extraction protocol surely can affect IPL distributions; as shown by Lengger et al. (2012) for
199 smaller sediment samples.

200 IPL analyses by high-performance liquid chromatography-mass spectrometry (HPLC-MS) were
201 carried out initially in 2010/2011 and again in 2015 as instrument protocols improved. In between these
202 analyses we did not observe a notable selective loss of IPL compounds, instead we were able to detect a
203 much larger suite of IPL structures due to improved detection and chromatographic separation techniques
204 (Wörmer et al., 2013). The confidence in these results are supported by the analysis of IPL standards
205 (Suppl. Table 2) that are stored at -20°C over several years (fresh standard mixtures are typically prepared
206 every 2 to 3 years), which do not indicate degradation of any particular IPL over time (Suppl. Fig. 1).
207 The analysis in 2010/2011 focused on absolute concentrations of the major IPLs (for distinction between
208 major and minor IPLs see results section). Aliquots of the TLE were dissolved in DCM/methanol (5:1
209 v/v) for injection on a ThermoFinnigan Surveyor HPLC system coupled to a ThermoFinnigan LCQ

210 DecaXP Plus ion-trap MS via electrospray interface (HPLC-ESI-IT-MSⁿ) using conditions described
211 previously (Sturt et al., 2004; Xie et al., 2014). Ten μ L of a known TLE aliquot spiked with C₁₉-PC as
212 internal standard was injected onto a LiChrosphere Diol-100 column (150 \times 2.1 mm, 5 μ m, Alltech,
213 Germany) equipped with a guard column of the same packing material. Absolute IPL concentrations
214 were determined in positive ionization mode with automated data-dependent fragmentation of the two
215 most abundant base peak ions. Acyl moieties of glycolipids and aminolipids were identified via HPLC-
216 IT-ESI-MS² experiments in positive ionization mode, whereas phospholipid side chain composition was
217 analyzed in negative ionization mode. Details of mass spectral interpretation, and identification of fatty
218 acid moieties are described in Sturt et al. (2004) and Schubotz et al. (2009) and are exemplified in Suppl.
219 Table 3. HPLC-MS analysis is not able to differentiate between double bonds or rings, therefore in the
220 subsequent text we will refer to double bond equivalents (DBE) to include both possibilities, similarly
221 absolute chain length cannot be determined as branched and straight chain alkyl chains cannot be
222 differentiated, therefore we report total carbon atom numbers for the alkyl side chains. Assignment of
223 the betaine lipid DGTS was according to the retention time of the commercially available standard DGTS
224 (Avanti Polar Lipids, USA). The isomer DGTA, which elutes at a different retention time due to its
225 structural difference (e.g., Brandsma et al., 2012) was not observed in the HPLC-MS chromatograms.
226 For all analyses, response factors of individual IPLs relative to the injection standard C₁₉-PC were
227 determined using dilution series of commercially available standards (Suppl. Table 2).

228 Subsequent analyses in 2015 were used to obtain sum formulas and IPL structures based on exact
229 masses in the MS1 and MS-MS experiments and to additionally provide data on minor lipids, which were
230 below detection limit during the 2010/2011 ion trap analyses (for distinction between major and minor

231 lipids see results section). For these measurements absolute quantities could not be determined since the
232 TLE had been used for other experiments and the information on TLE amounts used was unknown;
233 therefore, these analyses are used to describe relative abundances. Analyses were performed on a Bruker
234 maXis Plus ultra-high resolution quadrupole time-of-flight mass spectrometer (Q-TOF) with an ESI
235 source coupled to a Dionex Ultimate 3000RS UHPLC. Separation of IPLs was achieved using a Waters
236 Acquity UPLC BEH Amide column as described in Wörmer et al. (2013), which resulted in better
237 chromatographic separation of compounds and higher sensitivity compared to the 2010/2011 analyses.
238 Relative proportions of compounds were quantified taking the different response factors of IPL classes
239 into account. Peak areas in extracted mass chromatograms were corrected with absolute response factors
240 determined in dilution series of commercially available standards (Suppl. Table 2). Some ions assigned
241 to either PE-AEG and PC-AEG could not be quantified individually due to co-elution of these compounds
242 and were thus quantified as one group using the mean response factor of PE- and PC-DAG. For
243 compound classes for which no standards were available, (e.g., PI-DAG, OL and the unknown aminolipids
244 AL-I and AL-II) the relative responses could not be corrected for. Assuming these compounds may
245 ionize similarly as structurally related IPLs, values may be off by a factor of 0.2 to 1.4, which is the
246 maximum range of response factors observed for the standards.

247

248 *2.4 Statistical analysis*

249 Nonmetric multidimensional scaling (NMDS) analysis was used to illustrate the relationships
250 among objects hidden in a complex data matrix (Rabinowitz, 1975) and was performed in the free software
251 R (version 3.4.3, www.r-project.org/) with *metaMDS* (vegan library, version 2.4-6) as described by

252 Wakeham et al. (2012). The datasets of relative lipid distribution and variations in carbon number and
253 double bond equivalents were standardized by Hellinger transformation using the function *decostand*,
254 while for all other variables (environmental parameters, microbial groups) absolute numbers were used.
255 The compositional dissimilarity was calculated by Euclidean distance measure. The resulting plot shows
256 the distribution of lipids and sampling depths. Microbial groups and geochemical parameters were
257 overlaid by function *envfit*. Lower stress is related to high quality of solution, and stress values ≤ 0.1
258 indicate results of good quality (Rabinowitz, 1975). Non-parametric Spearman Rank Order Correlation
259 analysis was performed on combined data of environmental variables and IPL ratios and IPL relative
260 abundances of all four stations using SigmaPlot 11.0 (Systat Software Inc., San Jose, USA).

261

262 **3. Results**

263 *3.1 Biogeochemical setting*

264 All along the transect, the thin mixed layer (upper ~20 m) was warm, ~25–28 °C, with oxygen
265 concentrations approaching air saturation at ~200 μM (Fig. 2). The euphotic zone (1% of surface
266 photosynthetically active radiation) generally ranged between 50 and 80 m depth. The thermocline was
267 abrupt at ~20–50 m, where temperatures dropped to ~15–18 °C and oxygen decreased to ~20 μM .
268 Temperatures stabilized by ~250–300 m depth at ~10–12 °C and oxygen levels were $<2 \mu\text{M}$; especially
269 at Station 8 there were spatially and temporally variable oxygen intrusions into the upper portion of the
270 OMZ. By ~600–800 m depth, a deep oxycline was observed where oxygen concentrations began to rise
271 again to ~40 μM at temperatures of ~4 °C by 1250 m. For the purposes of this discussion, the water
272 column of the ETNP was partitioned into four horizons based on oxygen content: an oxic epipelagic zone

273 down to the thermocline (0–50 m; $200 \mu\text{M} > \text{O}_2 > 20 \mu\text{M}$); an upper OMZ (Station 1 and 8: 50–300 m,
274 Station 5: 50 – 350 m, Station 2: 50–200 m; $20 \mu\text{M} > \text{O}_2 > 2 \mu\text{M}$); the core OMZ (Station 1 and 8: 300–
275 800 m, Station 5: 350 – 600 m Station 2: 200 – 600 m; $\text{O}_2 < 2 \mu\text{M}$); and a deep oxycline (Station 1 and 8
276 ≥ 800 m, Station 2 and 5 ≥ 600 m; $\text{O}_2 > 2 \mu\text{M}$) of rising O_2 levels (Fig. 1a). Note that sampling at stations
277 1 and 8 reached to 1250 m depth so SPM from >750 m depth best represents the deep oxycline.

278 Chl- α was highest in surface waters with maximum values of $1.8 \mu\text{g/L}$ at 10 m at station 5, was
279 between 0.2 and $0.7 \mu\text{g/L}$ at station 1, 2 and 8 and decreased to values close to zero below 100 m at all
280 stations (Fig. 2; see also Fiedler and Talley, 2006, and Pennington et al., 2006, for additional results from
281 previous surveys). HPLC analysis of accessory pigments (Goericke et al., 2000; Ma et al., 2009) showed
282 that picoplankton, primarily *Prochlorococcus* (indicated by divinyl chlorophyll α), were an important
283 component of the photoautotrophic community, along with diatoms (fucoxanthin), especially *Rhizosolenia*
284 at the deep fluorescence maximum at stations 1 and 5 but *Chaetoceros* at station 8, and prymnesiophytes
285 (19'hexanoyloxyfucoxanthin and 19'butanoyloxyfucoxanthin; DiTullio and Geesey, 2002; Suppl. Table
286 4). High phaeopigment abundances (up to 90% of [Chl- α + phaeopigments]) attested to algal senescence
287 or grazing by macro- (Wishner et al., 2013; Williams et al. 2014) and micro-zooplankton (Olson and Daly,
288 2013) above and into the oxycline. Primary maxima in transmissivity corresponded with the peak Chl-
289 α concentrations and fluorescence maxima, but secondary transmissivity maxima between 300 and 400 m
290 at stations 1, 5, and 8 indicated elevated particle abundances in the core of the OMZ (Fig. 2).

291 Nitrite (NO_2^-) maxima in the OMZ at all stations coincided with nitrate (NO_3^{2-}) deficits (Fig. 3).
292 Ammonium (NH_4^+) concentrations changed little through the water column (Fig. 3). Phosphate (PO_4^{3-} ;
293 Fig. 3) and total dissolved nitrogen (TDN; not shown) were low (respectively, < 0.5 and $< 3 \mu\text{M}$) in the

294 upper 20 m of the oxic zone, but increased in the OMZ. High PO_4^{3-} (up to 3.4 μM) and high TDN (up
295 to 44.5 μM) were observed in the deep OMZ at stations 2, 5 and 8 (Fig. 3). N:P ratios were lower than
296 the Redfield ratio (16) at all sites and depths (Fig. 3); N:P minima were lowest in surface waters (2.6 to
297 10 in the upper 20 m) and at ~500 m within the core OMZ and the deep oxycline at station 1 (<9).

298 POC and TN concentrations (< 53 μm material) were highest in the euphotic zone (POC: 20 – 100
299 $\mu\text{g/L}$; TN: 4 – 15 $\mu\text{g/L}$), rapidly dropping to 5 $\mu\text{g/L}$ and 1 $\mu\text{g/L}$ below the upper OMZ, respectively (Fig.
300 2; Suppl. Fig. 2). Secondary maxima for POC (~10 $\mu\text{g/L}$) and TN (~2 $\mu\text{g/L}$) within the core of the OMZ
301 might reflect elevated microbial biomass there. Concentrations dropped in the deep oxycline to ≤ 3 $\mu\text{g/L}$
302 and ≤ 0.5 $\mu\text{g/L}$ for POC and TN, respectively.

303 Absolute IPL concentrations were determined by ion trap LCMS and varied between 250 and 1500
304 ng/L in the oxic zone and abruptly decreased more than 10-fold (to <20 ng/L) in the upper OMZ (Fig. 2).
305 Secondary maxima in IPL concentrations (15–40 ng/L) within the OMZ at all stations roughly coincided
306 with elevated numbers of prokaryotes (Fig. 2). IPL:POC ratios decreased with increasing depth (Fig. 2),
307 tracking trends of POC, TN and IPL concentrations.

308

309 *3.2 Changes in IPL composition with water column depth in the ETNP*

310 In total, 24 IPL classes were identified in the ETNP (Fig. 4, Suppl. Fig. 3). Eleven major and thirteen
311 minor IPL classes were detected in the QTOF analyses, which were classified according to their relative
312 abundance: if an individual IPL comprised more than 10% of total IPLs at any depth of the four stations
313 it was classified as a major IPL, compounds <10% were minor IPLs. Based on their head group
314 composition IPLs were grouped into glycolipids, phospholipids or aminolipids. Figure 3 shows changes

315 in the relative abundances (as percentages of total IPLs, excluding isoprenoidal archaeal IPLs) of
316 glycolipids, phospholipids and aminolipids as well as several substitute lipid ratios, reflecting preferential
317 biosynthesis of non-phosphorus lipids to replace phospholipids under phosphate-limiting growth (cf. Van
318 Mooy et al., 2006; Popendorf, et al., 2011b; Carini et al., 2015; Bosak et al., 2016). Relative abundances
319 of non-isoprenoidal phospholipids were highest in the core OMZ between 400 and 600 m at all sites,
320 where they comprise up to 45–76% at stations 1, 2 and 5 and between 12 and 61% at station 8.
321 Phospholipid abundances were lower within the upper OMZ and oxic zone at all stations (between 4 and
322 55%) and in the deep oxycline at station 8 (<1%). Aminolipid content was highest in SPM from the
323 upper 55 m at station 5 and 8 (10 to 25%), the core OMZ at station 8 (15 to 34%) and the deep oxycline
324 at station 1 (17%). Lower aminolipid contents (2 to 11%) were observed in the oxic zone and the core
325 OMZ at stations 1 and 2, the upper OMZ at station 5 (0 to 11%) and the deep oxycline at station 8 (<2%).
326 Glycolipid abundance was >9% at all depths, with highest abundance (average 54%, max. 82%) within
327 the upper OMZ and oxic zone at all stations and the deep oxycline at station 8. Values down to 9% were
328 observed within the core OMZ.

329

330 *3.2.1 Major lipids*

331 The eleven major IPL classes included three IP-GDTs of archaeal origin: (1G-GDGT, 2G-GDGT and
332 HPH-GDGT); and eight IPLs assigned to either a bacterial or eukaryotic origin: three glycolipids (1G-
333 DAG, 2G-DAG, SQ-DAG), four phospholipids (PG-DAG, PE-DAG, PC-DAG, PE+PC-AEG) and one
334 aminolipid (DGTS). All major lipid classes were found at almost all depths at all four stations, but with
335 varying relative abundances (as % of total IPL; Fig. 4, Suppl. Table 1).

336 *Archaeal IP-GDGTs*: Relative abundances of archaeal IPL (IP-GDGTs) generally increased with
337 depth from non-detectable in surface waters to >50% of total IPLs at station 8 (bottom of core OMZ and
338 deep oxycline). Archaeal IP-GDGT abundances at stations 1 and 2 peaked at 30% (bottom of upper
339 OMZ, core OMZ and deep oxycline) but were generally <10% at station 5 (Fig. 4). At station 1 and 2,
340 1G-GDGT and 2G-GDGT were most abundant with variable amounts of HPH-GDGTs, whereas 1G-
341 GDGT and HPH-GDGT dominated archaeal IPLs at station 5 and 8 at most depths. Distributions of
342 glycosidic IPL-GDGTs obtained in the present investigation corroborate the absolute values reported by
343 (Xie et al., 2014) for stations 1 and 8: 1G-GDGT was more abundant than 2G-GDGT at station 8 when
344 compared to station 1. The core GDGTs of 1G-GDGTs and HPH-GDGTs are dominated by GDGT-0
345 and crenarchaeol (Suppl. Fig. 4), whereas 2G-GDGTs are dominated by GDGT-2 and a small amount of
346 crenarchaeol (Zhu et al., 2016)

347 *Diacylglycerol lipids*: The oxic zone and the upper OMZ were dominated (~50–80% of IPL) at all
348 sites by the diacylglycerol glycolipids, 1G-DAG, 2G-DAG and SQ-DAG (Fig. 4). In the core OMZ and
349 deep oxycline, relative amounts of 2G-DAG and SQ-DAG decreased to 4% and 12%, respectively. 1G-
350 DAG abundances were lowest in the core OMZ at all stations, but were up to 47% of total IPL in the deep
351 oxycline. Diacylglycerol phospholipids, PE-, PG- and PC-DAG, were the second most abundant IPLs.
352 Abundances of PE- and PG-DAG were highest within the upper and core OMZ, constituting >50% in the
353 core OMZ at station 1, >30% at stations 2 and 5, and 16% at station 8. PC-DAG, with average
354 abundances of 5% at stations 1, 2, 8 and 3% at station 5, did not exhibit depth-related trends. The third
355 most abundant diacylglycerol class was the betaine lipid DGTS, which was present throughout the water
356 column at average abundances of 7% at station 1, 2 and 8, and 5% at station 5.

357 Major diacylglycerol lipids showed changes in average number of carbon atoms and double bond
358 equivalents (DBE) with depth (Fig. 5, Suppl. Table 5). The glycolipids and PC-DAG decreased in average
359 carbon number by up to three carbons and decreased in DBE by up to 2 at the top of the upper OMZ and
360 within the core OMZ compared to the oxic zone and the deep oxycline. Average carbon numbers for
361 PE- and PG-DAG and DGTS showed an inverse trend, both generally increasing up to two carbons
362 between the upper OMZ and the core OMZ. Changes in DBE were not as pronounced for PG-DAG and
363 DGTS, on average 1 to 2 DBE greater in surface waters than in deeper waters, while the number of DBE
364 increased on average with depth for PE-DAG.

365 *Acyl-ether glycerol lipids:* Mixed ether-ester glycerol core structures with either PE or PC head
366 groups were observed at all stations and all depths (generally 4-12%) except for the deep oxycline at
367 station 8.

368

369 3.2.2 Minor lipids

370 Thirteen minor IPL classes were identified, five of which were glycolipids, four phospholipids and
371 four aminolipids. All minor lipid classes were detected at each site except for OH-DGTS which was
372 absent at station 1. Some minor lipids were found at all depths, whereas others were restricted to specific
373 depth zones as defined by oxygen content (Fig. 4).

374 *Diacylglycerol lipids:* Two minor diacylglycerol glycolipids, 1G-OH-DAG and 3G-DAG, were
375 most abundant within the oxic zone and the upper OMZ, comprising between 2 to 15% of minor lipids on
376 average (0.1 to 0.6% of total IPLs), but were only sporadically found within the core OMZ and deep
377 oxycline. 1G-OH-DAG showed highest relative abundances at station 5, constituting up to 40% of minor

378 lipids. Four additional phospholipids with diacylglycerol core structures with the following head groups
379 were identified: diphosphatidylglycerol (DPG), phosphatidyl-(*N*)-methylethanolamine (PME),
380 phosphatidyl-(*N,N*)-dimethylethanolamine (PDME) and phosphatidyl inositol (PI). DPG, PME-DAG and
381 PDME-DAG had highest relative abundances (respectively 65, 56 and 35% of minor IPL) within the upper
382 and core OMZ, but at lower abundances within the oxic zone at all stations and in the deep oxycline at
383 stations 1, 2 and 5. PI-DAG was most abundant in the oxic zone and the upper OMZ (up to 25% of
384 minor IPL), but was also present in the core OMZ and the deep oxycline, except for station 8. Three
385 types of aminolipids were observed as minor lipids. OH-DGTS with up to three hydroxyl-groups
386 attached to the fatty acyl side chains (Suppl. Fig. 5) was observed at most depths at station 8 with an
387 average relative abundance of 23% among the minor lipids; it was also occasionally detected at stations 2
388 and 5 within the oxic zone and upper OMZ. Two additional aminolipids had an undefined head group
389 that exhibited fragmentation patterns characteristic of betaine lipids, but without established betaine head
390 group fragments (Suppl. Fig. 6b, c). The tentatively assigned sum formula for the head group of the first
391 unknown aminolipid (AL-I) at ca. 6.7 minutes LC retention time was $C_8H_{17}NO_3$ and for the second
392 unknown aminolipid (AL-II) at 10.5 minutes was $C_7H_{15}NO_3$. The head group sum formula for AL-II
393 matches that of DGCC, but the diagnostic head group fragment of *m/z* 252 was not detected, and
394 furthermore, AL-II did not elute at the expected earlier retention time for DGCC. AL-I and AL-II were
395 detected at most depths at all four stations, with average abundances of 1 to 6% of the minor lipids for
396 AL-I and comparably higher relative abundances ranging from 16 to 36% for AL-II.

397 *Acyl-ether glycerol lipid:* One minor compound that eluted slightly earlier than SQ-DAG had a
398 fragmentation pattern similar to SQ-DAG but with exact masses of the parent ion and MS-MS fragments

399 in both positive and negative ion mode that suggested a mixed acyl-ether glycerol core lipid structure
400 (Suppl. Fig. 6 d, e). Tentatively assigned as SQ-AEG, this IPL was observed at most depths at all four
401 stations with highest relative abundances of 5 to 60% of minor IPLs within the oxic zone.

402 *Sphingolipids:* Two types of sphingolipids were identified, monoglycosyl ceramide (1G-CER), and
403 hydroxylated monoglycosyl ceramide (1G-OH-CER) with up to two hydroxyl groups attached to the
404 hydrophobic side chains (Suppl Fig. 5e). Both were observed at all depths at stations 1, 2, and 5 at
405 average relative abundances between 3 and 8% of minor IPLs, but neither was detected in the deeper part
406 of the core OMZ or deep oxycline at station 8.

407 *Ornithine lipids:* Trace amounts (<4%) of ornithine lipids were detected in the core OMZ of stations
408 2 and 5.

409

410 3.2.3 Statistical relationships between environmental parameters and lipid distribution

411 Spearman Rank Order Correlation was used to evaluate relationships between relative lipid
412 abundance of lipid classes and environmental parameters (Table 1). The glycolipids 2G- and SQ-DAG
413 showed highly significant ($p < 0.001$) and positive correlations with depth, fluorescence, POC, TN,
414 temperature and Chl- α , significant positive correlations were also observed with oxygen. Both also
415 showed highly significant but negative correlations with phosphate and nitrate, and these overall trends
416 were mirrored in the SQ-DAG:PG-DAG ratio. Total glycolipids (GL) and 1G-DAG only showed
417 correlations with a few environmental parameters and total GL were only significantly positively
418 correlated with oxygen. Most aminolipids and phospholipids did not show significant correlations with
419 environmental parameters and any other correlations were neither strongly positive nor negative.

420 Relative abundances of total aminolipids and aminolipid (AL) to phospholipid (PL) ratios correlated
421 positively with ammonium. AL:PL also correlated positively with oxygen. Relative abundance of total
422 phospholipids and most individual phospholipids (PG-, PE-, PME-, and PDME-DAG) correlated
423 negatively with oxygen. The only phospholipid that significantly correlated with phosphate was PDME,
424 however, the positive correlation is not strong ($r^2 < 0.4$).

425 NMDS analysis revealed that all samples from the oxic zone had a negative loading on the NMDS2
426 axis along with environmental variables such as oxygen, fluorescence, TN, POC and Chl- α . IPLs with
427 a strong negative loading on the NMDS2 axis (< -0.2) were 1G-OH-DAG, SQ-AEG, 2G-DAG, SQ-DAG,
428 PI-DAG and OH-DGTS. Most samples from the core OMZ and deep oxycline had a positive loading on
429 the NMDS2 axis, together with depth, phosphate and nitrate. IPLs that showed a strong positive loading
430 on the NMDS2 axis (> 0.2) were PDME-DAG, 2G-GDGT, DPG, PME-DAG and HPH-GDGT. Almost
431 all environmental variables had low p -values (< 0.001), indicating highly significant fitted vectors with the
432 exception of temperature, salinity, ammonium and nitrate. Highest goodness of fit statistic was observed
433 with oxygen ($r^2 = 0.54$), followed by phosphate ($r^2 = 0.48$) and then fluorescence ($r^2 = 0.46$).

434

435 **4. Discussion**

436 The moderate primary productivity in surface waters of the ETNP, intense microbial degradation of
437 particulate organic matter exported to the thermocline, and restricted midwater oxygen replenishment
438 produce the strong, shallow (~20 m deep) oxycline and a ~500 m thick OMZ with dissolved oxygen
439 concentrations of $< 2 \mu\text{M}$, not unlike other oceanic OMZs (e.g., Ulloa et al., 2012). The ETNP is
440 dominated by picoplankton, and micro-grazers reported consuming most phytoplankton production

441 (Landry et al., 2011; Olsen and Daly, 2013). Peak macrozooplankton biomass was located at the
442 thermocline, near the upper boundary of the OMZ, but a secondary biomass peak of a different
443 zooplankton assemblage was present at the deep oxycline once O₂ concentrations rose to ~2 μM (Wishner
444 et al., 2013). Shallow-water, plankton-derived particulate organic carbon is the primary food source for
445 zooplankton in the mixed layer, upper oxycline and core OMZ, whereas deep POC, some of which might
446 have been produced by microbes in the OMZ, is important for deep oxycline zooplankton (Williams et al.,
447 2014). Microbial community structure and activities are typical of other OMZs (Taylor et al., 2001; Lin
448 et al., 2006; Woebken et al., 2007; Wakeham et al., 2007; 2012). Cell numbers of total prokaryotes were
449 highest in the euphotic layer and decreased with depth at the thermocline but rose again within the core
450 OMZ (Podlaska et al., 2012). Elevated rates of chemoautotrophy, measured by dark dissolved inorganic
451 carbon (DIC) assimilation, were observed at several depths in the OMZ and in the lower oxycline.
452 Transfer of chemoautotrophically-fixed carbon into zooplankton food webs is also evident (Williams et
453 al., 2014). Bacteria dominate the prokaryotic community at all stations. Nitrifying bacteria constituted
454 3-7% of total DAPI-positive prokaryotes in surface waters; sulfate-reducing bacteria (17 and 34% of total
455 prokaryotes), planctomycetes (up to 24% of total prokaryotes), and anammox bacteria (<1% of
456 prokaryotes) in the upper OMZ and deep oxycline might be associated with anoxic microzones within
457 particle aggregates even at low dissolved oxygen concentrations (Woebken et al., 2007; Carolan et al.,
458 2015). Archaeal cell abundances peaked at the start of the upper OMZ at all stations (up to 37% of total
459 prokaryotes at station 2), within the core OMZ at station 2 (up to 54% of total detected cells) and within
460 the deep oxycline at station 5 and 8 (around 25%; Fig. 2e). Crenarchaeota/thaumarchaeota represented
461 ~20% of prokaryotes throughout the water column, generally being highest in the lower OMZ and deep

462 oxycline, and at stations 2 and 5 just above the secondary Chl-*a* maxima at ~75 m. Euryarchaeota were
463 16-20% of total prokaryotes, especially in waters above the OMZ.

464 Total IPL concentrations that were over 50 times higher in the surface waters than at deeper depths
465 coincided with high Chl-*α* concentrations, reflecting the importance of phototrophic sources to the IPL
466 pool above the thermocline. Below the thermocline, IPL concentrations generally track trends in
467 microbial cell abundances, and elevated IPL concentrations in the upper and core OMZ coincide with
468 elevated nitrite concentrations. The rapid decrease in IPL concentrations below ~100 m probably results
469 from a combination of a dearth of potential source organisms and the decomposition of sinking detrital
470 lipids (Harvey et al., 1986; Matos and Pham-Thi, 2009). IPL concentration decreases below the euphotic
471 zone are well established (Van Mooy et al., 2006; Schubotz et al., 2009; Van Mooy and Fredricks, 2010;
472 Popenorf et al., 2011b; Wakeham et al., 2012). We believe that the diverse molecular compositions and
473 shifts in relative abundances of IPLs with changing geochemistry reflect a complex biological community
474 structure and their ecophysiologic adaptation throughout the water column.

475

476 *4.1 Provenance of IPLs in the ETNP*

477 Variations in IPL distributions and head group and core lipid compositions reflect the biogeochemical
478 stratification of the water column. Below we discuss potential sources of and possible physiological
479 roles for IPLs in the different zones.

480

481 *4.1.1 Oxic zone*

482 The glycosyldiacylglycerides that dominate the IPL composition in oxic surface waters, 1G-DAG,

483 2G-DAG and SQ-DAG, are major constituents of photosynthetic thylakoid and chloroplast membranes
484 (Wada and Murata, 1998; Siegenthaler, 1998) and are therefore generally assigned to photosynthetic algae
485 or cyanobacteria (Van Mooy et al., 2006; Pendorf et al., 2011b). These are also the likely predominant
486 sources in our study, however, notably 1G-DAG may also be synthesized by heterotrophic bacteria
487 (Pendorf et al., 2011a; Carini et al., 2015; Sebastian et al., 2016). In the oxic zone, 1G- and 2G-DAG
488 are predominantly comprised of C₁₆ and C₁₈ fatty acids with zero to 5 double bond equivalents
489 polyunsaturated acid (PUFA) combinations such as C_{16:4}/C_{18:3}, C_{16:4}/C_{18:4}, C_{18:3}/C_{16:2}, C_{18:4}/C_{14:0} and
490 C_{18:5}/C_{14:0} (Suppl. Table 5, Fig. 5). These are characteristic of eukaryotic algae (Brett and Müller-
491 Navarra, 1997; Okuyama et al., 1993), such as diatoms and prymnesiophytes that are the major eukaryotic
492 phytoplankton in the ETNP. SQ-DAG biosynthesized by cyanobacteria do not contain PUFA, but
493 instead predominantly contain combinations of C_{14:0}, C_{16:0}, and C_{16:1} fatty acids (e.g., Siegenthaler, 1998),
494 yielding shorter chain lengths and a lower average number of double bonds (0.5 to 1) than the other
495 glycolipids as observed at the ETNP (Fig. 5). Betaine lipids (DGTS) in surface waters of the ETNP are
496 comprised of C₁₄, C₁₆, C₁₈ and C₂₀ with multiple unsaturations or rings (on average 1.5 to 3 double bond
497 equivalents) and are also likely phytoplankton derived (Dembitsky, 1996; Pendorf et al., 2011a).

498 PC-DAG with fatty acyl combinations of C_{22:6} and C_{20:5} long-chain PUFA and C_{16:0} fatty acids (Suppl.
499 Table 5) in surface waters also point to primarily eukaryotic algal sources. PG-DAG is the only
500 phospholipid in cyanobacteria and thylakoid membranes of eukaryotic phototrophs (Wada and Murata,
501 1998). Heterotrophic bacteria are an additional source for PG-DAG since it can be a major phospholipid
502 in bacterial membranes (Goldfine, 1984). PE-DAG is a minor phospholipid in eukaryotic algae (e.g.,
503 Dembitsky et al., 1996) but is common in membranes of bacteria (Oliver and Colwell, 1973; Goldfine,

504 1984) and is biosynthesized by heterotrophic marine bacteria (Popendorf et al., 2011a). Lower average
505 number of double bond equivalents in PG- and PE-DAG (<2) in the upper water column of the ETNP are
506 consistent with a bacterial origin (Fig. 5).

507 Oxic ETNP waters contain PE- and PC-based phospholipids with mixed acyl and ether core lipids
508 (AEG), which are often referred to as 1-*O*-monoalkyl glycerol ethers (MAGE) if detected as core lipids.
509 PE-AEG have been described in some sulfate-reducing bacteria (Rütters et al., 2001), which in the oxic
510 zone or OMZ of the ETNP would require anoxic microzones in fecal pellets or aggregates (e.g., Bianchi
511 et al., 1992; Shanks and Reeder, 1993). In the ETNP, MAGE-based phospholipids were 1 to 30% of
512 total IPLs. MAGE, detected as core lipids in surface waters of the Southern Ocean and eastern South
513 Atlantic are thought to be breakdown products of IP-AEGs of aerobic bacterial origin (Hernandez-Sanchez
514 et al., 2014), but culturing experiments have yet to confirm this conclusion. Similarly, aerobic bacteria
515 (possibly cyanobacteria) are likely sources for SQ-AEG, since sulfoquinovosyl is a diagnostic headgroup
516 found in cyanobacteria, although, again, these lipids have not been reported in cultured cyanobacteria.
517 Other minor phospholipids in the euphotic zone include PI-DAG and DPG. They are minor components
518 in several marine algae (Dembitsky, 1996) and bacteria (Morita et al., 2010; Diervo et al., 1975;
519 Mileykovskaya and Dowhan, 2009). Bacteria may also be the source of the low detected levels of *N*-
520 methylated phospholipids PME-DAG and PDME-DAG (Goldfine and Ellis, 1964). 3G-DAG comprised
521 of C₁₄, C₁₆ and C₁₈ fatty acids with up to six double bond equivalents is another minor IPL detected in the
522 euphotic zone at all stations except for station 5. It has been found in some plants (Hölzl and Dörmann,
523 2007) and some anaerobic gram-positive bacteria (Exterkate and Veerkamp, 1969), which could both be
524 probable sources in the oxic euphotic zone of the ETNP.

525 The sphingolipid, 1G-CER, consists of a sphingosine backbone linked to a fatty acid via an amide
526 bond and was a minor component in the oxic zone (<5% of IPL) at all stations (Fig. 4). Glycosidic
527 ceramides occur in eukaryotic algae such as the coccolithophore *Emiliania huxleyi* (Vardi et al., 2009).
528 We also detected 1G-OH-CER with up to 2 hydroxylations in the core lipid structure (Suppl. Fig. 5).
529 Multiple-hydroxylated sphingoid bases are potential markers of viral infection and cell death in at least
530 some marine phytoplankton, notably *E. huxleyi* (Vardi et al., 2009). We did not, however, find mass
531 spectral evidence for the presence of viral polyhydroxylated 1G-CER, as described by Vardi et al. (2009)
532 and therefore rather suggest that eukaryotic algal cells are potential sources for the 1G-CER (Lynch and
533 Dunn et al., 2004) in surface waters of the ETNP. We also detected hydroxylated glycolipids (1G-OH-
534 DAG) and aminolipids (OH-DGTS) with up to two hydroxyl-groups or one hydroxyl group combined
535 with an epoxy or keto function attached to the acyl groups (Suppl. Fig. 5). The addition of hydroxyl
536 groups or general oxidation of fatty acids in plants, algae and yeast is a defense mechanism and response
537 to oxidative stress (Kato et al., 1984; Andreou et al., 2009). Hydroxy fatty acids, for example, are
538 intermediates in oxidative degradation of fatty acids (Lehninger, 1970), and since they are constituents of
539 structural biopolymers of many microorganisms (Ratledge and Wilkinson, 1988), they are present in
540 marine particulate matter (e.g., Wakeham, 1999), likely derived from membrane constituents of Gram-
541 negative bacteria, the most abundant bacteria in seawater (Rappé and Giovannoni, 2000).

542

543 4.1.2 Upper OMZ

544 Glycolipid abundance varied between 15 to 80% of total IPL within the upper OMZ below the
545 thermocline/oxycline. SQ-DAG and 2G-DAG exhibited strong decreases in relative and absolute

546 abundance below 125 m at all stations consistent with the decrease in their phototrophic biomass.
547 Number of carbon atoms in the core lipid chains and number of double bond equivalents of glycolipids
548 showed considerable variations within the upper OMZ (Fig. 5), indicating a different assemblage of source
549 organisms compared to the oxic zone. Likewise, decreasing carbon numbers and double bond
550 equivalents for PC-DAG and DGTS combined with a dominance by C₁₄, C₁₆ and C₁₈ saturated and
551 monounsaturated fatty acids (Suppl. Table 5) supports a shift from eukaryotic to bacterial sources. This
552 suggests the diverse proteobacteria in the upper OMZ may biosynthesize non-phosphorus substitute IPLs.
553 1G-DAG or DGTS are known to replace phospholipids, primarily PE-DAG and PC-DAG under
554 phosphorus limited growth (Geske et al., 2012; Carini et al., 2015; Sebastian et al., 2016; Yao et al., 2015),
555 including at the phosphate concentrations of 2 to 2.5 μ M in the upper OMZ. Sulfate-reducing
556 proteobacteria, which comprise up to 10% of the total bacteria in the ETNP (Podlaska et al., 2012) may
557 be candidate organisms for this phospholipid to glycolipid replacement (Bosak et al., 2016). Structures
558 of minor IPLs, AL-I and AL-II were not fully elucidated (see Suppl. Fig. 6) and their origins remain
559 uncertain. PME- and PDME-DAG, DPG, 1G-CER and 1G-OH-CER within the upper OMZ are
560 consistent with previous reports of their production by (unidentified) bacteria near redox boundaries in
561 other stratified water bodies (Schubotz et al., 2009; Wakeham et al., 2012).

562 Archaeal IPLs with glycosidic headgroups and tetraether core structures (1G- and 2G-GDGT)
563 comprised a greater proportion of the overall IPL pool within the upper OMZ than in surface waters.
564 Analysis of these same samples by Xie et al. (2014) first reported that concentrations of glycosidic GDGTs
565 peak in the ETNP roughly at depths where nitrite maxima are observed. IP-GDGTs with the hexose-
566 phosphate-hexose (HPH) headgroups and the core GDGT crenarchaeol (Suppl. Fig. 4) of thaumarchaeota

567 (Schouten et al., 2008; Elling et al., 2017) were most abundant at depths of nitrate maxima at all ETNP
568 stations, as they are in other oxygen-deficient water columns (e.g., Pitcher et al., 2011; Lengger et al.,
569 2012; Schouten et al., 2012; Sollai et al., 2015), although they were present at greater depths in the ENT
570 as well. The microbial enumerations by Podlaska et al. (2012) had shown previously that
571 thaumarchaeota (referred to as crenarchaeota) and euryarchaeota constitute almost equal amounts to <10%
572 of total cell number in the upper OMZ of the ETNP. It is also possible that uncultured marine Group II
573 euryarchaeota are additional sources for glycosidic GDGTs as has been suggested previously (Lincoln et
574 al., 2014; Zhu et al., 2016).

575

576 4.1.3 Core OMZ and deep oxycline

577 IPL distributions in the core OMZ and at the deep oxycline of the ETNP that were notably different
578 from the oxic zone and the upper OMZ are consistent with *in-situ* microbial origins. We choose to
579 discuss the core OMZ and deep oxycline together because, although oxygen concentrations are beginning
580 to rise in the deep oxycline, IPL compositions in both zones are similar and likely reflect similar
581 biogeochemical sources. Phospholipid abundance at all stations generally increased to over 50% (except
582 for station 8) at the expense of glycolipids. PE and PG-DAG are the most abundant phospholipids in the
583 core OMZ, along with PC-DAG and PE- and PC-AEG, DPG. PME and PDME-DAG are all common
584 lipids in α -, γ - and some β -proteobacteria (Oliver and Colwell, 1973; Goldfine, 1984) that are present in
585 the OMZ (Podlaska et al., 2012). Changes in phospholipids chain length and number of double bond
586 equivalents further support *in-situ* IPL production (Fig. 5). Fatty acid combinations for phospholipids
587 were dominated by saturated C_{14:0}, C_{15:0} and C_{16:0} and monounsaturated C_{16:0} C₁₇ and C_{18:0} (Suppl. Table

588 5); PUFA were generally of reduced abundance, and odd-numbered fatty acids increased in proportion.
589 In the case of PUFA, even though they may be biosynthesized by piezophilic aerobic deep-sea bacteria
590 (DeLong and Yayanos, 1986, Fang et al. 2003; Valentine and Valentine, 2004), either the microaerophilic
591 bacteria in the deep OMZ of the ETNP do not produce PUFA or these labile fatty acids are rapidly degraded
592 *in-situ* (DeBaar et al., 1983; Prahel et al., 1984; Neal et al., 1986).

593 Among glycolipids, 1G-DAG was most abundant at the deep OMZ/oxycline at stations 1 and 8; here
594 1G-DAG abundance actually increases over that of shallower depths. Carbon number and number of
595 double bond equivalents for glycolipids are again distinct from the surface waters, with on average 1 to 2
596 carbon atoms shorter chain lengths and 1 to 3 fewer double bonds (Fig. 5), supporting the notion that at
597 least some of these glycolipids are biosynthesized *in-situ* and not simply exported from the surface waters.
598 In particular, SQ-DAG in the core OMZ/oxycline contained odd-carbon numbered fatty acids (e.g.,
599 C_{15:0}/C_{16:0} and C_{14:0}/C_{15:0}) different from the cyanobacterial SQ-DAG in surface waters (Suppl. Table 5).
600 Some Gram-positive bacillus and firmicutes biosynthesize 1G, 2G- and SQ-DAG (Hölzl and Dörmann,
601 2007) and 1G-, 2G- and SQ-DAG in deeply buried Wadden Sea sediments are attributed to anaerobic
602 bacteria (Seidel et al., 2012). However, Gram-positive bacteria are generally not abundant in seawater.

603 The core OMZ/deep oxycline are particularly enriched in archaeal GDGT, notably 1G-GDGT and
604 HPH-GDGT, with predominantly GDGT-0 and crenarchaeol as core lipids (Suppl. Fig. 4). At stations 1
605 and 8 where sampling penetrated below ~800 m depth, 1G-GDGT and HPH-GDGT constitute up to ~60%
606 and ~22%, respectively, of total IPL. Significantly, the elevated abundances of 1G-GDGT and HPH-
607 GDGT at the bottoms of the sampling depth profiles in the deep oxycline of stations 1 and 8 correspond
608 to depths at which ammonium concentrations are higher than shallower in the core OMZ (Fig. 2).

609 Remineralization at the deep-oxycline might provide additional ammonium to drive thaumarchaeotal
610 ammonium oxidation and production of archaeal IPLs.

611

612 *4.2 Factors influencing IPL distribution in the ETNP*

613 *4.2.1 Factors affecting structural diversity of the core lipid composition*

614 IPL in the ETNP display considerable diversity not only in the headgroup but also core lipid types,
615 from diacylglycerol lipids with varying number of carbon atoms (likely chain lengths) and zero to multiple
616 double bond equivalents (likely reflecting the number of unsaturations), with or without hydroxylations
617 to mixed ether/ester glycerolipids, sphingolipids and ornithine lipids. Statistical analysis provides aids
618 in illuminating influences of environmental factors and microbial community structure on the lipid
619 composition in the water column of the ETNP. Changes in core alkyl lipid chain length and degree of
620 unsaturation are often associated with temperature (Neidleman, 1987), even at the range of temperatures
621 of the ETNP water column. However, NMDS analysis did not yield any strong correlations between
622 temperature and number of carbon atoms in the side chains or double bond equivalents of the major IPL
623 classes ($r^2 < 0.02$, Suppl. Table 6), nor with other environmental parameters ($r^2 < 0.3$, Suppl. Table 6).
624 Instead, changing biological sources may play a decisive role in determining number of carbon atoms and
625 double bond equivalents in the ETNP. For instance, long-chain PUFAs in surface waters are mainly
626 synthesized by phytoplankton, while in deeper waters some bacteria may biosynthesize these PUFAs.
627 The degree of hydroxylation in the acyl side chains also did not show any clear link to specific
628 environmental factors, although, both 1G-OH-CER and OH-DGTS had negative loadings on the NMDS-
629 2 axis indicating a higher abundance of these compounds in oxic samples. It is possible that hydroxylated

630 IPLs play a role during oxidative stress and/or are involved in other defense mechanisms (Kato et al.,
631 1984; Andreou et al., 2009).

632 Mixed ether-acyl lipids have been reported in various oceanic settings (Hernandez-Sanchez et al.,
633 2014). In our study, there was no noticeable correlation between PE- and PC-AEG and depth or oxygen
634 concentrations (Fig. 6). Ornithine lipids were strongly negatively loaded on the NMDS-1 axis, but none
635 of the measured environmental parameters could account for this negative loading (Fig. 6). Therefore,
636 it remains unclear what factor(s) ultimately determine their distribution. Likewise, there were no
637 significant correlations between the sphingolipid 1G-CER and any environmental parameter. Since
638 ether-acyl lipids, ornithine lipids and sphingolipids play many functional roles in biological systems, their
639 variable distribution within the water column reflect most likely the diversity of microbes inhabiting the
640 dynamic oxygen regime of the ETNP.

641

642 *4.2.2 Factors influencing head group composition*

643 NMDS analysis of normalized IPL composition and quantitative microbial data (abundance of α , β ,
644 γ , ϵ -proteobacteria, sulfate-reducing bacteria δ -proteobacteria, planctomycetes, crenarchaeota including
645 thaumarchaeota and euryarchaeota) did not yield any high goodness of fit statistic ($r^2 < 0.3$; Suppl. Table
646 6) that would clearly delineate specific prokaryotic sources for the various IPL. This absence of
647 statistical correlation would result if neither the IPL compositions of SPM nor the structure and lipid
648 composition of the prokaryotic community were sufficiently unique to strongly distinguish the
649 biogeochemical zones. Indeed, although there are depth-related differences in IPL composition of SPM
650 and prokaryotic community, there is considerable overlap. Therefore, instead of trying to elucidate

651 specific IPL sources, we here query the affect environmental factors such as temperature, nutrient or
652 oxygen concentrations may have on the IPL compositions in the ENTTP, and by analogy to natural marine
653 settings in general. Most the major and minor glycolipids were loaded negatively on the NMDS2 axis,
654 as were oxygen, fluorescence, Chl- α , POC and TN (Fig. 6). A notable exception was 1G-DAG which
655 had only a slightly negative loading on the NMDS-2 axis. These relationships (loadings) roughly reflect
656 the vertical distribution of IPLs in the water column of the ETNP. Glycolipids, particularly 2G-DAG
657 and SQ-DAG, were most abundant in the euphotic oxic zone characterized by high oxygen concentration
658 and moderate primary productivity, dominated by phytoplankton, primarily cyanobacteria (high POC, TN
659 and elevated Chl- α and fluorescence). Spearman Rank Order Correlations confirm these observations,
660 including the lack of significant correlations between 1G-DAG and depth or any other environmental
661 parameter. One explanation is that 1G-DAG originates from assorted sources throughout the water
662 column independent of any single environmental variable. Similarly, PC-DAG, PG-DAG, and DGTS
663 did not correlate with any of the tested environmental variables, because their compositions are relatively
664 homogeneous across all biogeochemical zones. PE-, PME- and PDME-DAG, and DPG, on the other
665 hand, that became more prevalent within the core OMZ, and at deeper depths where oxygen concentrations
666 decrease and nutrient (NO_3^- and PO_4^{3-}) concentrations were elevated due to organic matter
667 remineralization, gave positive loadings with these environmental parameters on the NDMS2 axis.
668 Archaeal IPLs showed positive loadings on the NMDS2 axis, consistent with the increasing importance
669 of archaeal abundance with depth and at reduced oxygen concentrations.

670

671 *4.2.3 Links between substitute lipid ratios and nutrient concentrations*

672 SQ-DAG and PC-DAG are often the most abundant respective glycolipids and phospholipids in the
673 surface ocean (Popendorf et al., 2011a,b), including the Eastern Tropical South Pacific (Van Mooy and
674 Fredricks, 2010). The abundance of SQ-DAG in the surface waters of the ETNP (18-50% of total IPL)
675 is thus not unusual. In the ETNP, however, PC-DAG was comparably minor (3-13% of total IPL).
676 Instead, DGTS was abundant at some stations, up to ~20% of major IPL at station 5. SQ-DAG and
677 DGTS serve similar biochemical functions as the phospholipids PG-DAG and PC-DAG, respectively, due
678 to similar ionic charges at physiological pH. The former may be preferentially biosynthesized by
679 phytoplankton and some bacteria as substitute lipids for PG-DAG and PC-DAG when phosphate starved
680 (Benning, 1993; Van Mooy et al., 2006, 2009). Likewise, 1G-DAG, glycuronic acid diacylglycerol
681 (GADG) and ornithine lipids may substitute for PE-DAG in marine bacteria (e.g., chemoheterotrophic α -
682 proteobacteria of the SAR11 clade of *Pelagibacter* sp.: Carini et al., 2015; the sulfate reducing bacterium,
683 *Desulfovibrio alaskensis*: Bosak et al., 2016). In oligotrophic surface waters of the Sargasso Sea (PO_4^{3-}
684 <10 nM) ratios of SQ-DAG:PG-DAG and DGTS:PC-DAG are high (4 to 13) compared to the same ratios
685 (3) in the phosphate replete South Pacific ($\text{PO}_4^{3-} >100$ nM), consistent with cyanobacteria synthesizing
686 phosphorus-free substitute lipids to maintain growth in response to phosphorus deprivation (Van Mooy et
687 al., 2009). At the ETNP, SQ-DAG:PG-DAG ratios ranged between 1 and 10 within the upper 100-200
688 m along the transect and were <1 deeper into the OMZ (Fig. 3). DGTS:PC-DAG ratios in the ETNP
689 were quite variable, ranging between 0.4 and 2.4 at most depths, but with notable spikes (>30) within the
690 oxic zone at station 5, within the upper core OMZ at station 2 and 8 and in the lower portion of the core
691 OMZ at station 8. 1G-DAG:PE-DAG ratios were highly variable (0.2 to 945) and were highest within
692 the upper OMZ at station 2, 5 and 8 and within the deep oxycline at station 8, where 1G-DAG:PE ratios

693 range between 290 and 945 (Fig. 3). To test the substitute lipid hypothesis for the ETNP, we performed
694 a Spearman Rank Order Correlation analysis of known substitute lipid ratios as well as total aminolipid
695 (AL) to phospholipid (PL) and total glycolipid (GL) to PL ratios with nutrient concentrations and other
696 environmental parameters. Only SQ-DAG:PG-DAG was significantly correlated with phosphate (-0.56,
697 $p < 0.001$) but also correlated with other parameters, such as depth (-0.76, $p < 0.001$) and oxygen
698 concentration (0.58, $p < 0.001$). These correlations reflect the elevated SQ-DAG:PG-DAG ratios (2-8) in
699 the surface waters and upper OMZ (Fig. 3) and support the notion that SQ-DAG might serve as a substitute
700 lipid in both surface waters and the OMZ when phosphate concentrations are in the low micromolar range
701 (~ 0.1 - $0.4 \mu\text{M}$ in surface waters; ~ 2 - $3.5 \mu\text{M}$ in the OMZ). Other proposed substitute lipid ratios,
702 DGTS:PC-DAG (Van Mooy et al., 2009) and 1G-DAG:PE-DAG (Carini et al., 2015), did not correlate
703 with nutrient concentrations in the water column of the ETNP but rather showed highly variable
704 distributions. Similarly, AL:PL ratios did not exhibit strong relationships with any environmental
705 parameter, and GL:PL ratios showed similar but less pronounced trends as SQ-DAG:PG-DAG ratios.
706 Overall, we observed no correlation between these substitute lipid ratios and phosphate concentration in
707 the ETNP. We propose that non-phosphorus IPL within the OMZ of the ETNP originate from bacteria
708 growing under low micromolar concentrations of phosphate. Indeed, the culture experiments of Bosak
709 et al. (2016) demonstrated that the sulfate reducer, *Desulfovibrio alaskensis*, begins to replace most of its
710 membrane phospholipids with 1G-DAG, glycuronic acid diacylglycerol and ornithine lipids even at
711 phosphate concentrations as high as $20 \mu\text{M}$.

712

713 **5. Conclusions**

714 The water column of the ETNP is characterized by a diverse suite of intact polar lipids. IPL
715 distributions reflect the dynamic nature of the biological community in the ETNP, with light and oxygen
716 as primary determinants, from fully oxygenated euphotic surface waters to an aphotic strong oxygen
717 minimum zone at mid-depth. Highest concentrations of IPLs (250 – 1500 ng/L) in oxygenated surface
718 waters zone results from abundant phototrophic eukaryotic and cyanobacterial sources above the OMZ.
719 Secondary peaks in IPL concentration (12 – 56 ng/L) within the core of the OMZ mirror elevated
720 abundances of heterotrophic and chemoautotrophic bacteria and archaea under low oxygen conditions.
721 Glycolipids derived from photoautotrophs generally accounted for more than 50% of total IPLs in the
722 euphotic zone (< 200 m, oxic and upper OMZ zones), but bacterial phospholipids were more abundant
723 (avg. 40%) in the OMZ and deep oxycline layers. Archaeal GDGTs were abundant within the OMZ and
724 deep oxycline, consistent with elevated archaeal abundances there. Variations in major fatty acid
725 constituents within IPL classes with acyl core moieties show that biological source(s) for the different IPL
726 were distinct in each depth/oxygen-content horizon. Nevertheless, microbial sources for many of the
727 detected lipids remain unclear and therefore potentially unique ecophysiological adaptations these lipids
728 may represent remain to be explored.

729 The presence of the glycolipid, monoglycosyl diacylglycerol (1G-DAG), and the betaine lipid,
730 diacylglyceryl homoserine (DGTS), both with varying fatty acid compositions, within all biogeochemical
731 zones, and especially in the OMZ, indicates that these canonical phototrophic markers are not only
732 biosynthesized in surface waters, but may indeed be produced in the aphotic water column and by a much
733 larger host of organisms than previously thought. Since 1G-DAG and DGTS can be biosynthesized by
734 various bacteria to replace phospholipids under phosphorus limited growth, we suggest that they serve as

735 non-phosphorus substitute lipids for some microorganisms in the OMZ. The presence of these substitute
736 lipids at micromolar concentrations of phosphate of the ETNP suggests that the paradigm of substitute
737 lipid biosynthesis being restricted to the PO_4^{3-} -depleted oligotrophic surface ocean may need to be re-
738 evaluated.

739

740 **Author contribution**

741 SGW collected the samples. SGW, FS and KUH designed the study. SX and FS measured and processed
742 the data. JSL and FS performed statistical analyses. FS and SGW wrote the paper with input from SX,
743 KUH and JSL.

744

745 **Competing interests**

746 The authors declare that they have no conflict of interest.

747

748 **Acknowledgments**

749 We are grateful to the captain and the crew of R/V *Seward Johnson*, to K. Daly and K. Wishner as co-
750 chief scientists, and to the U.S. National Science Foundation for supporting the cruise. H. Albrecht, B.
751 Olsen and S. Habtes helped with PM sampling. We thank K. Fanning and R. Masserini (University of
752 South Florida) for providing their nutrient results; C. Flagg (Stony Brook) processed CTD hydrographic
753 data; Jay Brandes and Mary Richards (Skidaway Institute) conducted the POC and TN analyses; B. Olson
754 and K. Daly (University of South Florida) provided ship-board Chl-*a* analyses; and G. DeTullio (College
755 of Charleston) conducted HPLC analyses of pigments. Lab supplies and analytical infrastructure for

756 lipid analyses was funded by the Deutsche Forschungsgemeinschaft (DFG, Germany) through the Cluster
757 of Excellence/Research Center MARUM. The UHPLC-QTOF instrument was granted by the DFG,
758 Germany through grants Inst 144/300-1. S. Xie was funded by the China Scholarship Council, F.
759 Schubotz by the Zentrale Forschungsförderung of the University of Bremen, and U.S. National Science
760 Foundation grant OCE-0550654 to S. G. Wakeham supported this project. SGW also acknowledges a
761 Fellowship from the Hanse-Wissenschaftskolleg (Hanse Institute for Advanced Studies) in Delmenhorst,
762 Germany.

763

764 **References**

765 Andreou, A., Brodhun, F., Feussner, I.: Biosynthesis of oxylipins in non-mammals, *Progr. Lip. Res.*, 48,
766 148-170, 2009.

767 Bale, N. J., Hopmans, E. C., Schoon, P. L., de Kluijver, A., Downing, J. A., Middelburg, J. J., Sinninghe
768 Damsté, J. S. and Schouten, S.: Impact of trophic state on the distribution of intact polar lipids in
769 surface waters of lakes. *Limnol. Oceanogr.*, 61, 1065–1077, 2016.

770 Basse, A., Zhu, C., Versteegh, G.J.M., Fischer, G., Hinrichs, K.-U., and Mollenhauer, G.: Distribution of
771 intact and core tetraether lipids in water column profiles of suspended particulate matter off Cape
772 Blank, NW Africa, *Org. Geochem.*, 72, 1-13, 2014.

773 Benning, C., Beatty, J. T., Prince, R. C., and Somerville C. R.: The sulfolipid
774 sulfoquinovosyldiacylglycerol is not required for photosynthetic electron transport in *Rhodobacter*
775 *sphaeroides* but enhances growth under phosphate limitation, *Proc. Natl. Acad. Sci. USA*, 90, 1561–
776 1565, 1993.

777 Bianchi, M., Marty, D., Teyssié, J.-L., and Fowler, S. W.: Strictly aerobic and anaerobic bacteria
778 associated with sinking particulate matter and zooplankton fecal pellets, *Mar. Ecol. Prog. Ser.*, 88, 55-
779 60, 1992.

780 Bosak, T., Schubotz, F., de Santiago-Torio, A., Kuehl, J. V., Carlson, H. K., Watson, N., Daye, M.,
781 Summons, R. E., Arkin, A. P., and Deutschbauer A. M.: System-wide adaptations of *Desulfovibrio*
782 *alaskensis* G20 to phosphate-limited conditions, *PLoS ONE* 11, e0168719, 2016.

783 Brandsma, J., Hopmans, E. C., Philippart, C. J. M., Veldhuis, M. J. W., Schouten, S., and Sinninghe
784 Damste, J. S.: Low temporal variation in the intact polar lipid composition of North Sea coastal marine
785 water reveals limited chemotaxonomic value, *Biogeosciences*, 9, 1073–1084, 2012.

786 Brett, M. T., and Müller-Navarra, D. C.: The role of highly unsaturated fatty acids in aquatic foodweb
787 processes, *Freshw. Biol.*, 38, 483–499, 1997.

788 Carini P., Van Mooy B. A. S., Thrash J. C., White A., Zhao Y., Campbell E. O., Fredricks H. F., and
789 Giovannoni S. J.: SAR11 lipid renovation in response to phosphate starvation. *Proc. Natl. Acad. Sci.*
790 *USA*, 112, 7767–7772, 2015.

791 Carolan, M.T., Smith, J.M., and Beman, J.M.: Transcriptomic evidence for microbial sulfur cycling in the
792 eastern tropical North Pacific oxygen minimum zone. *Front. Microbiol.* 6, 334, 2015.

793 Cass, C. J., and Daly, K. L.: Ecological characteristics of eucalanoid copepods of the eastern tropical
794 North Pacific Ocean: Adaptations for life within a low oxygen system, *J. Exp. Mar. Biol. Ecol.*, 468,
795 118-129, 2015.

796 Cavan, E. L., Trimmer, M., Shelley, F., Sanders, R.: Remineralization of particulate organic carbon in an
797 ocean oxygen minimum zone, *Nat. Comm.*, 8, 14847, 2016.

798 Codispoti, L. A., and Richards, F. A.: An analysis of the horizontal regime of denitrification in the eastern
799 tropical North Pacific. *Limnology and Oceanography* 21, 379-388, 1976.

800 DeBaar, H. J. W., Farrington, J. W. and Wakeham, S. G.: Vertical flux of fatty acids in the North Atlantic
801 Ocean, *J. Mar. Res.*, 41, 19-41, 1983.

802 DeLong, E. F. and Yayanos, A.: Biochemical function and ecological significance of novel bacterial lipids
803 in deep-sea prokaryotes, *Appl. Environ. Microbiol.*, 51, 730-737, 1986.

804 Dembitsky, V.: Betaine ether-linked glycerolipids: Chemistry and biology, *Progr. Lip. Res.*, 35, 1-51,
805 1996.

806 Diervo, A. J. and Reynolds, J. W.: Phospholipid composition and cardiolipin synthesis in fermentative
807 and nonfermentative marine bacteria, *J. Bacteriol.* 123, 294-301, 1975.

808 DiTullio, G., and Geesey, M. E.: Photosynthetic Pigments in Marine Algae and Bacteria. In: G Bitton (ed),
809 *Encyclopedia of Environmental Microbiology*, vol. 5, Wiley, pp 2453-2470, 2002.

810 Elling, F. J., Könneke, M., Mußmann, M., Greve, A., and Hinrichs, K.-U.: Influence of temperature, pH,
811 and salinity on membrane lipid composition and TEX86 of marine planktonic thaumarchaeal isolates,
812 *Geochim. Cosmochim. Acta*, 171, 238-255, 2015.

813 Elling, F. J., Könneke, M., Nicol, G. W., Stieglmeier, M., Bayer, B., Spieck, E., La Torre, De J. R., Becker,
814 K. W., Thomm, M., Prosser, J. I., Herndl, G. J., Schleper, C., and Hinrichs, K.-U. Chemotaxonomic
815 characterisation of the thaumarchaeal lipidome, *Environ. Microbiol.* 10, 1080, 2017.

816 Ertefai, T., Fisher, M., Fredricks, H. and Lipp, J.: Vertical distribution of microbial lipids and functional
817 genes in chemically distinct layers of a highly polluted meromictic lake, *Org. Geochem.*, 39, 1572-
818 1588, 2008.

819 Exterkate, F. A., and Veerkamp, J. H.: Biochemical changes in *Bifidobacterium bifidum* var.
820 *Pennsylvanicus* after cell wall inhibition. I. Composition of lipids, *Biochim. Biophys. Acta*, 176, 65–
821 77, 1969.

822 Fang, J., Kato, C., Sato, T., Chan, O., and McKay, D.: Biosynthesis and dietary uptake of polyunsaturated
823 fatty acids by piezophilic bacteria. *Comp. Biochem. Physiology Part B*, 137 455–46, 2004.

824 Fiedler, P. C., and Talley, L. D.: Hydrography of the eastern tropical Pacific: A review. *Progr. Oceanogr.*,
825 69, 143-180, 2006.

826 Franck, V. M., Smith, G. J., Bruland, K. W., and Brzezinski, M. A.: Comparison of size-dependent carbon,
827 nitrate and silicic acid uptake rates in high- and low-iron waters. *Limnol. Oceanogr.*, 50, 825-838,
828 2005.

829 Geiger, O., González-Silva, N., López-Lara, I. M., and Sohlenkamp, C.: Amino acid-containing
830 membrane lipids in bacteria, *Progr. Lip. Res.*, 49, 46–60, 2010.

831 Geiger, O., Röhrs, V., Weissenmayer, B., Finan, T. M., and Thomas-Oates, J. E.: The regulator gene *phoB*
832 mediates phosphate stress-controlled synthesis of the membrane lipid diacylglyceryl-N,N,N-
833 trimethylhomoserine in *Rhizobium* (*Sinorhizobium*) *meliloti*, *Mol. Microbiol.*, 32, 63–73, 1999.

834 Geske, T., Dorp vom, K., Dörmann, P., and Hölzl G.: Accumulation of glycolipids and other non-
835 phosphorous lipids in *Agrobacterium tumefaciens* grown under phosphate deprivation, *Glycobiol.*, 23,
836 69–80, 2012.

837 Goericke, R., Olson, R. J., and Shalapyonok, A.: A novel niche for *Prochlorococcus* sp. in low-light
838 suboxic environments in the Arabian Sea and the Eastern Tropical North Pacific, *Deep Sea Res. I*, 47,
839 1183-1205, 2000.

840 Goldfine, H.: Bacterial membranes and lipid packing theory, *J. Lip. Res.*, 25, 1501–1507, 1984.

841 Goldfine, H., and Ellis, M. E.: N-methyl groups in bacterial lipids, *J. Bacteriol.*, 87, 8–15, 1964.

842 Gruber, N.: The marine nitrogen cycle: overview and challenges, in: *Nitrogen in the marine environment*,
843 Eds. DG Capone, DA Bronk, MR Mulholland, EJ Carpenter, Burlington, MA, USA: Academic, 1-50,
844 2008.

845 Harvey, R. H., Fallon R. D., and Patton, J. S.: The effect of organic matter and oxygen on the degradation
846 of bacterial membrane lipids in marine sediments, *Geochim. Cosmochim. Acta*, 50, 795-804, 1986.

847 Hernandez-Sanchez, M. T., Homoky, W. B., and Pancost, R. D.: Occurrence of 1-O-monoalkyl glycerol
848 ether lipids in ocean waters and sediment, *Org. Geochem.* 66, 1–13, 2014.

849 Hölzl, G., and Dörmann, P.: Structure and function of glycolipids in plants and bacteria, *Progr.*
850 *Lip. Res.* 46, 225–243, 2007.

851 Hurley, S. J., Elling, F. J., Könneke, M., Buchwald, C., Wankel, S. D., Santoro, A. E., Lipp, J. S., Hinrichs,
852 K.-U., and Pearson, A.: Influence of ammonia oxidation rate on thaumarchaeal lipid composition and
853 the TEX86 temperature proxy, *Proc. Natl. Acad. Sci. USA*, 113, 7762-7767, 2016.

854 Kalvelage, T., Lavik, G., Jensen, M. M., Revsbech, N. P., Löscher, C., Schunck, H., Desai, D. K., Hauss,
855 H., Kiko, R., Holtappels, M., LaRoche, J., Schmitz, R. A., Graco, M. I., and Kuypers, M. M. M.:
856 Aerobic microbial respiration in oceanic oxygen minimum zones, *PLoS ONE*, 10(7):e0133526, 2015.

857 Karstensen, J., Stramma L., and Visbeck M.: Oxygen minimum zones in the eastern tropical Atlantic and
858 Pacific oceans, *Progr. Oceanogr.*, 77, 331-350, 2008.

859 Kato, T., Yamaguchi, Y., Hirano, T., and Yokoyama, T.: Unsaturated hydroxy fatty acids, the self
860 defensive substances in rice plant against rice blast disease, *Chem. Let.*, 409-412, 1984.

861 Keeling, R. F., Körtzinger, A., and Gruber N.: Ocean deoxygenation in a warming world, *Annu. Rev.*
862 *Marine. Sci.*, 2, 199–229, 2010.

863 Kharbush, J. J., Allen, A. E., Moustafa, A., Dorrestein, P.C., Aluwihare, L. I.: Intact polar diacylglycerol
864 biomarker lipids isolated from suspended particulate organic matter accumulating in an
865 ultraoligotrophic water column, *Org. Geochem.*, 100, 29-41, 2016.

866 Lam, P. and Kuypers, M. M. M.: Microbial nitrogen cycling processes in oxygen minimum zones, *Annu.*
867 *Rev. Marine. Sci.*, 3, 317–345, 2011.

868 Landry, M. R., Selph, K. E., Taylor, A.G., Décima, M., Balch, W. M., and Bidigare R. R.: Phytoplankton
869 growth, grazing and production balances in the HNLC equatorial Pacific, *Deep Sea Res. I*, 58, 524-
870 535, 2011.

871 Lavín, M. F., Fiedler, P. C., Amador, J. A., Balance, L. T., Färber-Lorda, J., Mestas-Nuñez, A. M.: A
872 review of eastern tropical Pacific oceanography: Summary, *Progr. Oceanogr.*, 69, 391-398, 2006.

873 Lee C., and Cronin C.: Particulate amino acids in the sea: Effects of primary productivity and biological
874 decomposition, *J. Mar. Res.*, 42, 1075-1097, 1984.

875 Lehninger A. L.: Oxidation of fatty acids, in: *Biochemistry*, New York: Worth, 417-432, 1970.

876 Lengger, S. K., Hopmans, E. C., Sinninghe Damsté, J. S., and Schouten, S.: Comparison of extraction and
877 work up techniques for analysis of core and intact polar tetraether lipids from sedimentary
878 environments, *Org. Geochem.*, 47, 34–40, 2012.

879 Lin, X., Wakeham, S. G., Putnam, I. F., Astor, Y. M., Scranton, M. I., Chistoserdov, A. Y., and Taylor, G.
880 T.: Comparison of vertical distributions of prokaryotic assemblages in the anoxic Cariaco Basin and
881 Black Sea by use of fluorescence in situ hybridization, *Appl. Environ. Microbiol.*, 72, 2679-2690,

882 2006.

883 Lincoln, S. A., Wai, B., Eppley, J. M., Church, M. J., Summons, R. E. and DeLong, E. F.: Planktonic
884 Euryarchaeota are a significant source of archaeal tetraether lipids in the ocean, *Proc. Natl. Acad. Sci.*
885 *USA*, 111, 9858–9863, 2014.

886 Lynch, D. V., and Dunn, T. M.: An introduction to plant sphingolipids and a review of recent advances in
887 understanding their metabolism and function, *New Phytol.*, 161, 677-702, 2004.

888 Ma, Y., Zeng, Y., Jiao, N., Shi, Y., and Hong, N.: Vertical distribution and phylogenetic composition of
889 bacteria in the Eastern Tropical North Pacific Ocean, *Microbiol. Res.*, 164, 624-663, 2009.

890 Maas, A. E., Frazar, S. L., Outram, D.M., Seibel, B. A., and Wishner, K. F.: Fine-scale vertical
891 distributions of macroplankton and micronekton in the Eastern Tropical North Pacific in association
892 with an oxygen minimum zone, *J Plankt. Res.*, 36, 1557-1575, 2014.

893 Martin, J. H., Knauer, G. A., Karl, D. M., and Broenkow, W. W.: VERTEX: carbon cycling in the northeast
894 Pacific, *Deep-Sea Research* 34, 267-285, 1987.

895 Matos, A. R., and Pham-Thi, A.-T.: Lipid deacylating enzymes in plants: Old activities, new genes. *Plant*
896 *Physiol. and Biochem.* 47, 491-503, 2009.

897 Meador, T. B., Gagen, E. J., Loscar, M. E., Goldhammer, T., Yoshinaga, M. Y., Wendt, J., Thomm, M.,
898 and Hinrichs, K.-U.: *Thermococcus kodakarensis* modulates its polar membrane lipids and elemental
899 composition according to growth state and phosphate availability, *Front. Microbiol.*, 5:10,
900 doi:10.3389/fmicb.2014.00010, 2014.

901 Mileykovskaya, E., and Dowhan, W.: Cardiolipin membrane domains in prokaryotes and eukaryotes,
902 *Biochim. Biophys. Acta* 1788, 2084–2091, 2009.

903 Morita, Y. S., Yamaryo-Botte, Y., and Miyanagi, K.: Stress-induced synthesis of phosphatidylinositol 3-
904 phosphate in mycobacteria, *J. Biol. Chem.* 285, 16643-16650, 2010.

905 Neal, A. C., Prahl, F. G., Eglinton, G., O'Hara, S. C. M., and Corner, E. D. S.: Lipid changes during a
906 planktonic feeding sequence involving unicellular algae, Elminius Nauplii and Adult Calanus, *J. Mar.*
907 *Biol. Assoc. UK*, 66, 1-13, 1986.

908 Neidleman, S. L.: Effects of temperature on lipid unsaturation: Biotechnology and Genetic Engineering
909 *Reviews*, 5:1, 245-268, 1987.

910 Oliver, J. D., and Colwell, R. R.: Extractable lipids of gram-negative marine bacteria: Phospholipid
911 composition, *J. Bacteriol.* 114, 897-908, 1973.

912 Olson, M. B., and Daly, K. L.: Micro-grazer biomass, composition and distribution across prey resource
913 and dissolved oxygen gradients in the far eastern tropical north Pacific Ocean, *Deep Sea Res. I*, 75,
914 28-38, 2014.

915 Okuyama, H., Kogame, K., and Takeda, S.: Phylogenetic significance of the limited distribution of
916 octadecapentaenoic acid in prymnesiophytes and photosynthetic dinoflagellates, *Proc. NIPR Symp.*
917 *Polar Biol.*, 6, 21–26, 1993.

918 Parsons, T. R., Takahashi, M., and Hargrave B. (Eds.): *Biological Oceanographic Processes*, 3rd ed.,
919 Pergamon Press, NY, 1984.

920 Paulmier, A., and Ruiz-Pino, D.: Oxygen minimum zones (OMZs) in the modern ocean, *Progr. Oceanogr.*
921 80, 113-128, 2009.

922 Pennington, J. T., Mahoney, K. L., Kuwahara, V. S., Kolber, D. D., Cienes, R., Chavez, F. P.: Primary
923 production in the eastern tropical Pacific: A review, *Progr. Oceanogr.*, 69, 285-317, 2006.

924 Pitcher, A., Villanueva, L., Hopmans, E. C., Schouten, S., Reichart, G.-J. and Sinninghe Damsté, J. S.:
925 Niche segregation of ammonia-oxidizing archaea and anammox bacteria in the Arabian Sea oxygen
926 minimum zone, *ISME J.*, 5, 1896–1904, 2011.

927 Podlaska, A., Wakeham, S. G., Fanning, K. A., and Taylor, G. T.: Microbial community structure and
928 productivity in the oxygen minimum zone of the eastern tropical North Pacific, *Deep-Sea Res. Part I*,
929 66, 77–89, 2012.

930 Pependorf, K., Lomas, M., and Van Mooy, B.: Microbial sources of intact polar diacylglycerolipids in the
931 Western North Atlantic Ocean, *Org. Geochem.* 42, 803-811, 2011a.

932 Pependorf, K. J., Tanaka, T., Pujo-Pay, M., Lagaria, A., Courties, C., Conan, P., Oriol, L., Sofen, L. E.,
933 Moutin, T., and Van Mooy, B. A. S.: Gradients in intact polar diacylglycerolipids across the
934 Mediterranean Sea are related to phosphate availability, *Biogeosci.* 8, 3733–3745, 2011b.

935 Prahl, F. G., Eglinton, G., Corner, E. D. S., O'Hara, D. C. M., and Forsberg, T. E. V.: Changes in plant
936 lipids during passage through the gut of *Calanus*, *J. Mar. Biol. Assoc. UK*, 1984.

937 Rabinowitz, G. B.: An introduction to nonmetric multidimensional scaling, *Amer. J. Polit. Sci.*, 343-90,
938 1975.

939 Rappé, M. S., and Giovannoni, S. J.: The uncultured microbial majority, *Annu. Rev. Microbiol.*, 57, 369-
940 394, 2003.

941 Rojas-Jiménez, K., Sohlenkamp, C., Geiger, O., Martínez-Romero, E., Werner, D., and Vinuesa, P.: A
942 CIC chloride channel homolog and ornithine-containing membrane lipids of rhizobium tropici
943 CIAT899 are involved in symbiotic efficiency and acid tolerance, *Mol. Plant-Microbe Interact.*, 18,
944 1175–1185, 2005.

945 Rush, D., Wakeham, S. G., Hopmans, E. C., Schouten, S., and Damsté, J. S. S.: Biomarker evidence for
946 anammox in the oxygen minimum zone of the Eastern Tropical North Pacific, *Org. Geochem.*, 53,
947 80–87, 2012.

948 Rütters, H., Sass, H., Cypionka, H., and Rullkötter, J.: Monoalkylether phospholipids in the sulfate-
949 reducing bacteria *Desulfosarcina variabilis* and *Desulforhabdus amnigenus*, *Arch. Microbiol.*, 176,
950 435–442, 2011.

951 Schouten, S., Pitcher, A., Hopmans, E. C., Villanueva, L., Van Bleijswijk, J., and Sinninghe Damsté, J.
952 S.: Intact polar and core glycerol dibiphytanyl glycerol tetraether lipids in the Arabian Sea oxygen
953 minimum zone: I. Selective preservation and degradation in the water column and consequences for
954 the TEX86, *Geochim. Cosmochim. Acta*, 98, 228–243, 2012.

955 Schubotz, F., Wakeham, S. G., Lipp, J., Fredricks, H. F., and Hinrichs, K.-U.: Detection of microbial
956 biomass by intact polar membrane lipid analysis in the water column and surface sediments of the
957 Black Sea, *Environ. Microbiol.*, 11, 2720-2734, 2009.

958 Sebastian, M., Smith, A. F., González, J. M., Fredricks, H. F., Van Mooy, B., Koblížek, M., Brandsma,
959 J., Koster, G., Mestre, M., Mostajir, B., Pitta, P., Postle, A. D., Sánchez, P., Gasol, J. M., Scanlan, D.
960 J., and Chen, Y.: Lipid remodelling is a widespread strategy in marine heterotrophic bacteria upon
961 phosphorus deficiency, *ISME J*, 10, 968–978, 2016.

962 Seibel, B.A.: Critical oxygen levels and metabolic suppression in oceanic oxygen minimum zones, *J. Exp.*
963 *Biol.*, 214, 326-336, 2011.

964 Seidel, M., Graue, J., Engelen, B., Köster, J., Sass, H., and Rullkötter, J.: Advection and diffusion
965 determine vertical distribution of microbial communities in intertidal sediments as revealed by

966 combined biogeochemical and molecular biological analysis, *Org. Geochem.*, 52, 114–129, 2012.

967 Shanks, A. L., and Reeder, M. L.: Reducing microzones and sulfide production in marine snow. *Marine*
968 *Ecology Press Series 96*, 43-47, 1993.

969 Siegenthaler P.-A.: Molecular organization of acyl lipids in photosynthetic membranes of higher plants,
970 in: *Lipids in Photosynthesis*, Siegenthaler, P.-A., and Murata, N. (Eds). Dordrecht, the Netherlands:
971 Kluwer Academic Publishers, 119–144, 1998.

972 Sohlenkamp, C., López-Lara, I. M., and Geiger, O.: Biosynthesis of phosphatidylcholine in bacteria, *Progr.*
973 *Lip. Res.*, 42, 115–162, 2003.

974 Sollai, M., Hopmans, E. C., Schouten, S., Keil, R. G., and Sinninghe Damsté, J.S.: Intact polar lipids of
975 Thaumarchaeota and anammox bacteria as indicators of N cycling in the eastern tropical North Pacific
976 oxygen-deficient zone, *Biogeosci.*, 12, 4833-4864, 2015.

977 Stevens H., and Ulloa, O.: Bacterial diversity in the oxygen minimum zone of the eastern tropical South
978 Pacific, *Environ. Microbiol.*, 10, 1244–1259, 2008.

979 Stramma, L., Johnson, G. C., Sprintall, J., and Mohrholz, V.: Expanding Oxygen-Minimum Zones in the
980 Tropical Oceans, *Science*, 320, 655-658, 2008.

981 Stramma, L., Schmidtko, S., Levin, L. A., and Johnson, G. C.: Ocean oxygen minima expansions and their
982 biological impacts, *Deep Sea Res. I*, 57, 587-595, 2010.

983 Sturt, H. F., Summons, R. E., Smith, K.E., Elvert, M., Hinrichs, K.-U.: Intact polar membrane lipids in
984 prokaryotes and sediments deciphered by high-performance liquid chromatography/electrospray
985 ionization multistage mass spectrometry - new biomarkers for biogeochemistry and microbial ecology,
986 *Rapid Comm. Mass Spec.*, 18, 617-628, 2004.

987 Taylor, G. T., Iabichella, M., Ho, T.-Y., Scranton, M. I., Thunell, R. C., Muller-Karger, F., and Varela R.:
988 Chemoautotrophy in the redox transition zone of the Cariaco Basin: A significant midwater source of
989 organic carbon production, *Limnol. Oceanogr.*, 46, 148-163, 2001.

990 Tiano, L., Garcia-Robledo, E., Dalsgaard, T., Devol, A. H., Ward, B. B., Ulloa, O., Canfield, D. E., and
991 Revsbech, N. P.: Oxygen distribution and aerobic respiration in the north and south eastern tropical
992 Pacific oxygen minimum zones, *Deep Sea Res. I*, 94, 173-183, 2014.

993 Turich, C., and Freeman, K. H.: Archaeal lipids record paleosalinity in hypersaline systems, *Org.*
994 *Geochem.* 42, 1147-1157, 2011.

995 Ulloa, O., Canfield, D., DeLong, E. F., Letelier, R. M., and Stewart, F. J.: Microbial oceanography of
996 anoxic oxygen minimum zones, *Proc. Natl. Acad. Sci., USA* 109, 15996-16003, 2012.

997 Valentine, R. C., and Valentine, D. L.: Omega-3 fatty acids in cellular membranes: a unified concept,
998 *Progr. Lip. Res.* 43, 383–402, 2004.

999 Van Mooy, B. A. S., and Fredricks, H. F.: Bacterial and eukaryotic intact polar lipids in the eastern
1000 subtropical South Pacific: Water-column distribution, planktonic sources, and fatty acid composition,
1001 *Geochim. Cosmochim. Acta*, 74, 6499–6516, 2010.

1002 Van Mooy, B. A. S., Fredricks, H. F., Pedler, B. E., Dyhrman, S. T., Karl, D. M., Koblížek, M., Lomas,
1003 M. W., Mincer, T. J., Moore, L. R., Moutin, T., Rappé, M. S., and Webb, E. A.: Phytoplankton in the
1004 ocean use non-phosphorus lipids in response to phosphorus scarcity, *Nature*, 458, 69–72, 2009.

1005 Van Mooy, B. A. S., Rocap, G., Fredricks, H. F., Evans, C. T., and Devol, A. H.: Sulfolipids dramatically
1006 decrease phosphorus demand by picocyanobacteria in oligotrophic marine environments, *Proc. Natl.*
1007 *Acad. Sci. USA*, 103, 8607–8612, 2006.

1008 Vardi, A., Van Mooy, B. A. S., Fredricks, H. F., Pependorf, K. J., Ossolinski, J. E., Haramty, L., and Bidle,
1009 K. D.: Viral glycosphingolipids induce lytic infection and cell death in marine phytoplankton, *Science*,
1010 326, 861-865, 2009.

1011 Wada, H., and Murata, N.: Membrane Lipids in cyano- bacteria, in: *Lipids in Photosynthesis: Structure,*
1012 *Function and Genetics*, Siegenthaler, P., and Murata, N. (Eds), Dordrecht, the Netherlands: Kluwer
1013 Academic Publishers, 65–81, 1998.

1014 Wakeham, S. G., Turich, C., Schubotz, F., Podlaska, A., Li, X. N., Varela, R., Astor, Y., Sáenz, J. P.,
1015 Rush, D., Sinninghe Damsté, J. S., Summons, R. E., Scranton, M. I., Taylor, G. T., and Hinrichs, K.-
1016 U.: Biomarkers, chemistry and microbiology show chemoautotrophy in a multilayer chemocline in
1017 the Cariaco Basin, *Deep Sea Res. Part I*, 63, 133–156, 2012.

1018 Wakeham, S. G., Amann, R., Freeman, K. H., Hopmans, E. C., Jørgensen, B. B., Putnam, I. F., Schouten,
1019 S., Sinninghe Damsté, J. S., Talbot, H. M., and Woebken, D.: Microbial ecology of the stratified water
1020 column of the Black Sea as revealed by a comprehensive biomarker study, *Org. Geochem.*, 38, 2070–
1021 2097, 2007.

1022 Wakeham, S. G.: Monocarboxylic, dicarboxylic and hydroxy acids released by sequential treatments of
1023 suspended particles and sediments of the Black Sea, *Org. Geochem.* 30, 1059-1074, 1999.

1024 Wakeham, S. G.: Reduction of stenols to stanols in particulate matter at oxic-anoxic boundaries in sea
1025 water, *Nature*, 342, 787-790, 1989.

1026 Wakeham, S. G., and Canuel, E. A.: Organic geochemistry of particulate matter in the eastern tropical
1027 North Pacific Ocean: Implications for particle dynamics, *J. Mar. Res.*, 46, 182-213, 1988.

1028 Wakeham, S. G.: Steroid geochemistry in the oxygen minimum zone of the eastern tropical North Pacific

029 Ocean, *Geochim. Cosmochim. Acta*, 51, 3051-3069, 1987.

030 Williams, R. L., Wakeham, S., McKinney, R., Wishner, K. F.: Trophic ecology and vertical patterns of
031 carbon and nitrogen stable isotopes in zooplankton from oxygen minimum zone regions, *Deep Sea*
032 *Res. I*, 90 36-47, 2014.

033 Wishner, K. F., Outram, D. M., Seibel, B. A., Daly, K. L., and Williams, R. L.: Zooplankton in the eastern
034 tropical north Pacific: Boundary effects of oxygen minimum zone expansion, *Deep Sea Res. I*, 79,
035 122-140, 2013.

036 Wishner, K. F., Gelfman, C., Gowing, M. M., Outram, D. M., Rapien, M., and Williams, R. L.: Vertical
037 zonation and distributions of calanoid copepods through the lower oxycline of the Arabian Sea oxygen
038 minimum zone, *Progr. Oceanogr.*, 78, 163-191, 2008.

039 Wobken, D., Fuchs, B. M., Kuypers, M. M. M, and Aman, R.: Potential interactions of particle-associated
040 anammox bacteria with bacterial and archaeal partners in the Namibian upwelling system, *Appl.*
041 *Environ. Microbiol.*, 73, 4648-4657, 2007.

042 Wörmer, L., Lipp, J. S., Schröder, J. M., and Hinrichs, K.-U.: Application of two new LC-ESI-MS
043 methods for improved detection of intact polar lipids (IPLs) in environmental samples, *Org. Geochem.*
044 59, 10–21, 2013.

045 Wright, J. J., Konwar, K. M., and Hallam, S. J: Microbial ecology of expanding oxygen minimum zones,
046 *Nat. Rev. Microbiol.* 10, 381-394, 2012.

047 Xie, S., Liu, X.-L., Schubotz, F., Wakeham, S. G., and Hinrichs K.-U.: Distribution of glycerol ether lipids
048 in the oxygen minimum zone of the Easter Tropical North Pacific Ocean, *Org. Geochem.* 71, 60–71,
049 2014.

- 050 Yao, M., Elling, F. J., Jones, C., Nomosatryo, S., Long, C. P., Crowe, S. A., Antoniewicz, M. R., Hinrichs,
051 K.-U., and Maresca, J. A.: Heterotrophic bacteria from an extremely phosphate-poor lake have
052 conditionally reduced phosphorus demand and utilize diverse sources of phosphorus, *Environ.*
053 *Microbiol.* 18, 656–667, 2015.
- 054 Zavaleta-Pastor, M., Sohlenkamp, C., Gao, J. L., Guan, Z., Zaheer, R., Finan, T. M., Raetz, C. R. H.,
055 López-Lara, I. M., and Geiger, O.: *Sinorhizobium meliloti* phospholipase C required for lipid
056 remodeling during phosphorus limitation, *Proc. Natl. Acad. Sci. USA*, 107, 302–307, 2010.
- 057 Zhang, Y.-M., and Rock, C. O.: Membrane lipid homeostasis in bacteria, *Nat. Rev. Microbiol.*, 6, 222–
058 233, 2008.
- 059 Zhu, C., Wakeham, S. G., Elling, F. J., Basse, A., Mollenhauer, G., Versteegh, G. J. M., Könneke, M.,
060 and Hinrichs, K.-U.: Stratification of archaeal membrane lipids in the ocean and implications for
061 adaptation and chemotaxonomy of planktonic archaea, *Environ. Microbiol.* 18, 4324-4336, 2016.

062

.063 **Tables**

.064 **Table 1.** Spearman Rank Order Correlation coefficients (r) for data combined from all four stations. Only
.065 significant correlations, where $p < 0.05$ (highly significant $p < 0.001$, in bold), are presented.

	Glycolipids					Aminolipids					Phospholipids					
	% GL	% 1G	% 2G	% SQ	GL:PL	SQ:PG	% AL	% DGTS	AL:PL	DGTS:PC	% PL	% PC	% PG	% PE	% PME	% PDME
Depth	-0.32	-0.7	-0.67	-0.41	-0.76											
Fluorescence		0.63	0.67		0.65											
POC		0.61	0.6		0.6											
TN		0.66	0.62		0.63											
Oxygen	0.57	0.3	0.48	0.35	0.55	0.58		0.36			-0.49	-0.38	-0.33	-0.46	-0.52	
Temperature	0.3	0.52	0.63	0.39	0.69											
Chl a	0.35	0.72	0.71	0.42	0.78											-0.33
Phosphate		-0.62	-0.53	-0.4	-0.56											0.36
Nitrate		-0.53	-0.49		-0.38											
Nitrite		-0.33														0.3
Ammonium							0.41	0.42	0.35	0.4						
N:P		-0.3	-0.32													-0.36

Abbreviations: GL – glycolipids, 1G – monoglycosyl, 2G – diglycosyl, SQ – sulfoquinovosyl, PL – phospholipids, AL – aminolipids, DGTS – diacylglycerol trimethyl homoserine, PC – phosphatidyl choline, PG – phosphatidyl glycerol, PE – phosphatidyl ethanolamine, PME – phosphatidyl methyl-ethanolamine, PDME – phosphatidyl dimethyl-ethanolamine

067 **Figures**

068 **Figure 1.** a) Map of ETNP with R/V *Seward Johnson* (November 2007) cruise sampling stations
069 investigated in this study.

070

071 **Figure 2.** Depth profiles of (a) oxygen and temperature, (b) chlorophyll- α and transmissivity, (c)
072 particulate organic matter (POC) and C:N, (d) intact polar lipid (IPL) to POC ratio and IPL concentration,
073 and (e) absolute cell abundance and relative proportions of archaeal cells (data from Podlaska et al. (2012)).
074 C:N (SPM) is total carbon over total nitrogen of the solid phase collected by water filtration. Note that
075 C:N, POC and IPL/POC are only analyzed for $<53 \mu\text{m}$ particle fraction. Also depicted are the different
076 geochemical zones in the water column.

077

078 **Figure 3.** Depth profiles of (a) nitrate, nitrite, and ammonium, (b) phosphate and N:P, (c) total non-
079 archaeal (non-isoprenoidal) phospholipids, glycolipids and (d) aminolipids shown as percent of total intact
080 polar lipids and ratios of non-phospholipids to phospholipids for DGTS to PC-DAG (e) SQ-DAG to PG-
081 DAG, (e), and 1G-DAG to PE-DAG. Also depicted are the different geochemical zones in the water
082 column.

083

084 **Figure 4.** Relative abundance of (a) major and (b) minor IPLs at sampled depths of stations 1, 2, 5, and 8
085 in the ETNP. Major IPLs are defined as those comprising more than 10% of total IPLs (minor compounds
086 comprised less than 10%) at more than one depth horizon at the four stations. Also depicted are the
087 different geochemical zones in the water column.

.088

.089 **Figure 5.** Changes in average carbon atoms (CA) and number of double bond equivalents (DB) of the
.090 alkyl side chains of major IPLs detected at stations 1, 2, 5 and 8 in the ETNP.

.091

.092 **Figure 6.** Nonmetric multidimensional scaling (NMDS) ordination plot assessing the relationship between
.093 IPL biomarkers, sampling depths and geochemical parameters in the ETNP (stress=0.125). Squares
.094 represent the water depth of each sample and are color-coded according to the defined geochemical
.095 zonation. Filled circles stand for lipid distribution of major IPLs and open circles for minor IPLs on the
.096 ordination. Vector lines of geochemical parameters are weighted by their p-values with each NMDS axis.

.097

fig01

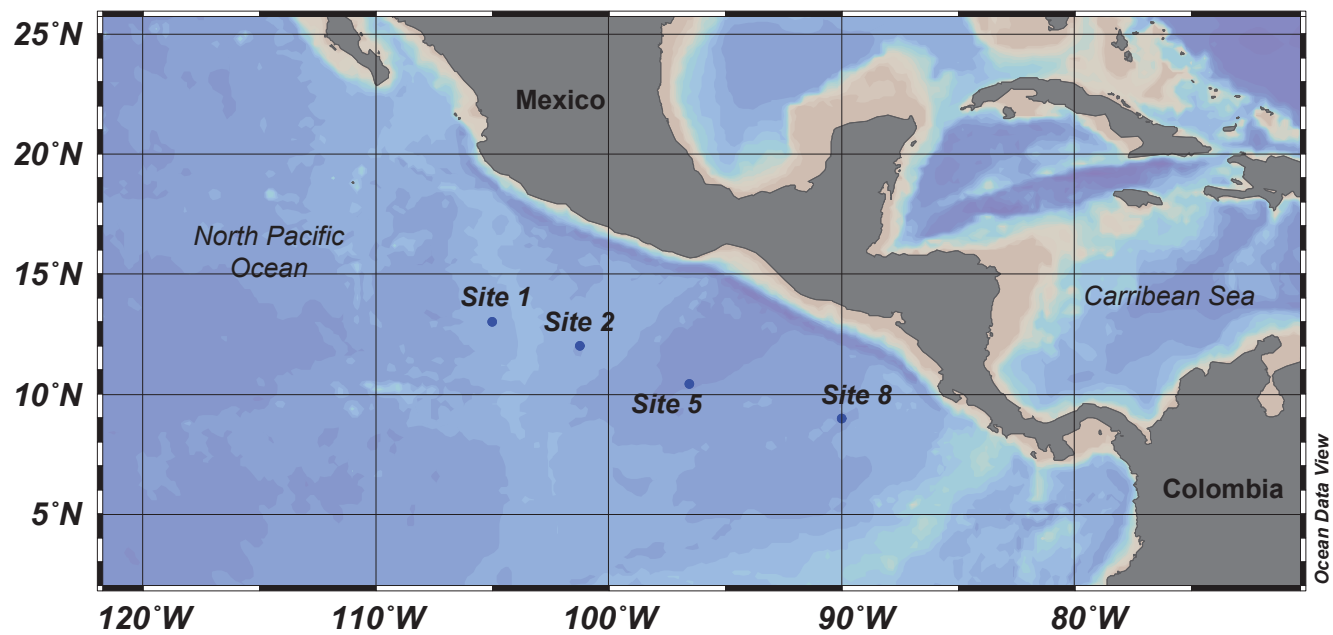


fig02

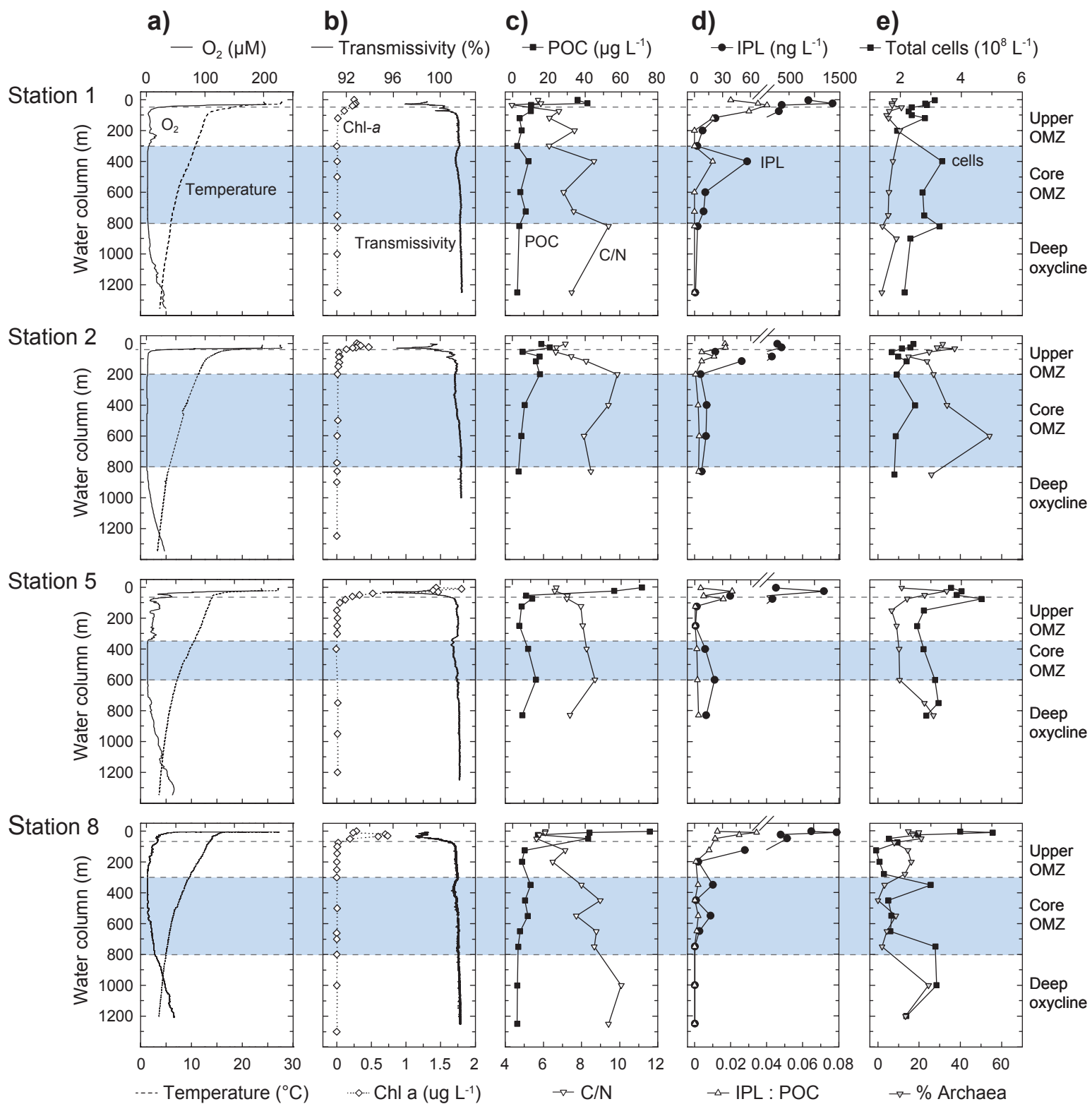


fig03

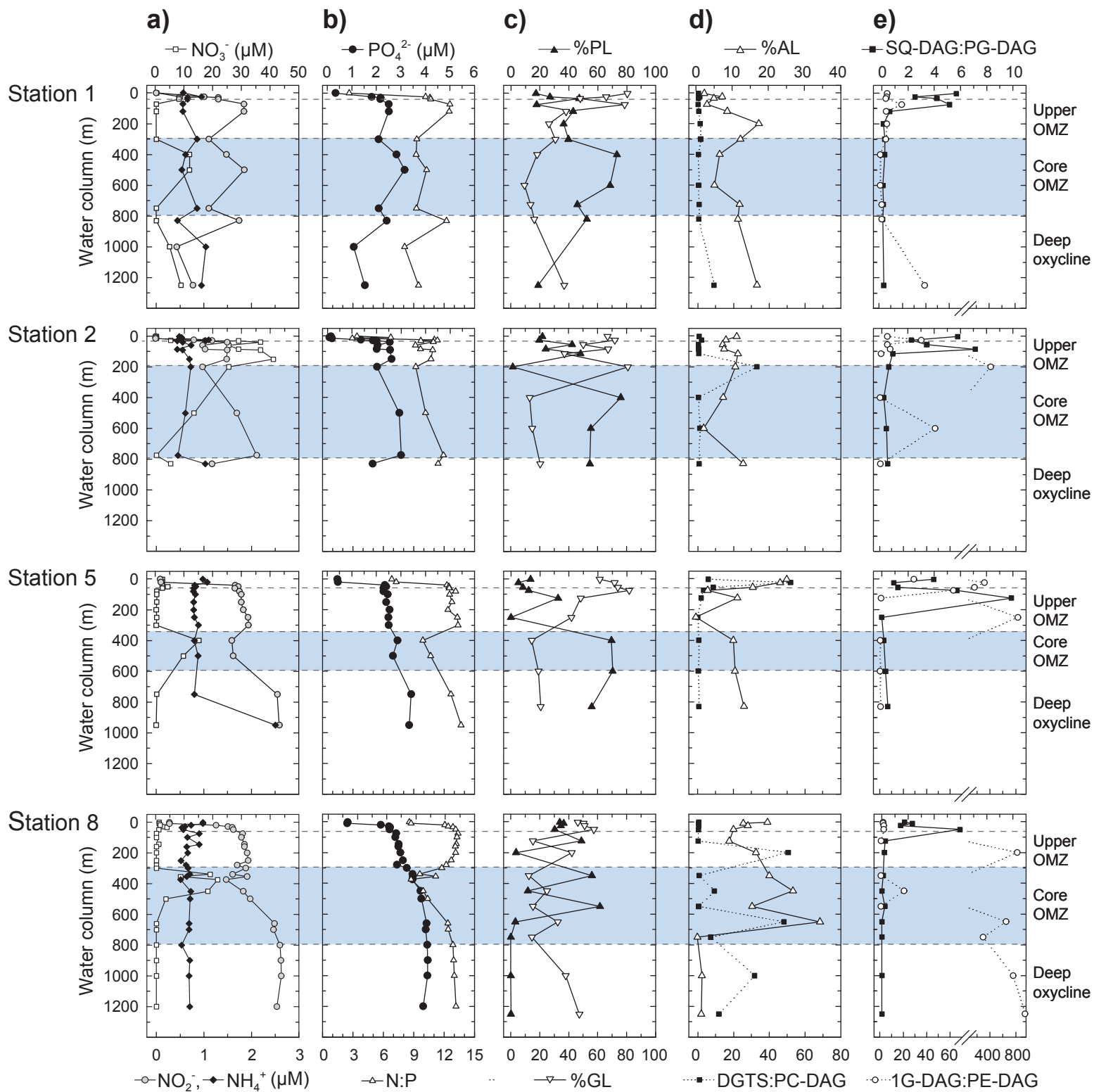


Figure 3

Major compounds

Minor compounds

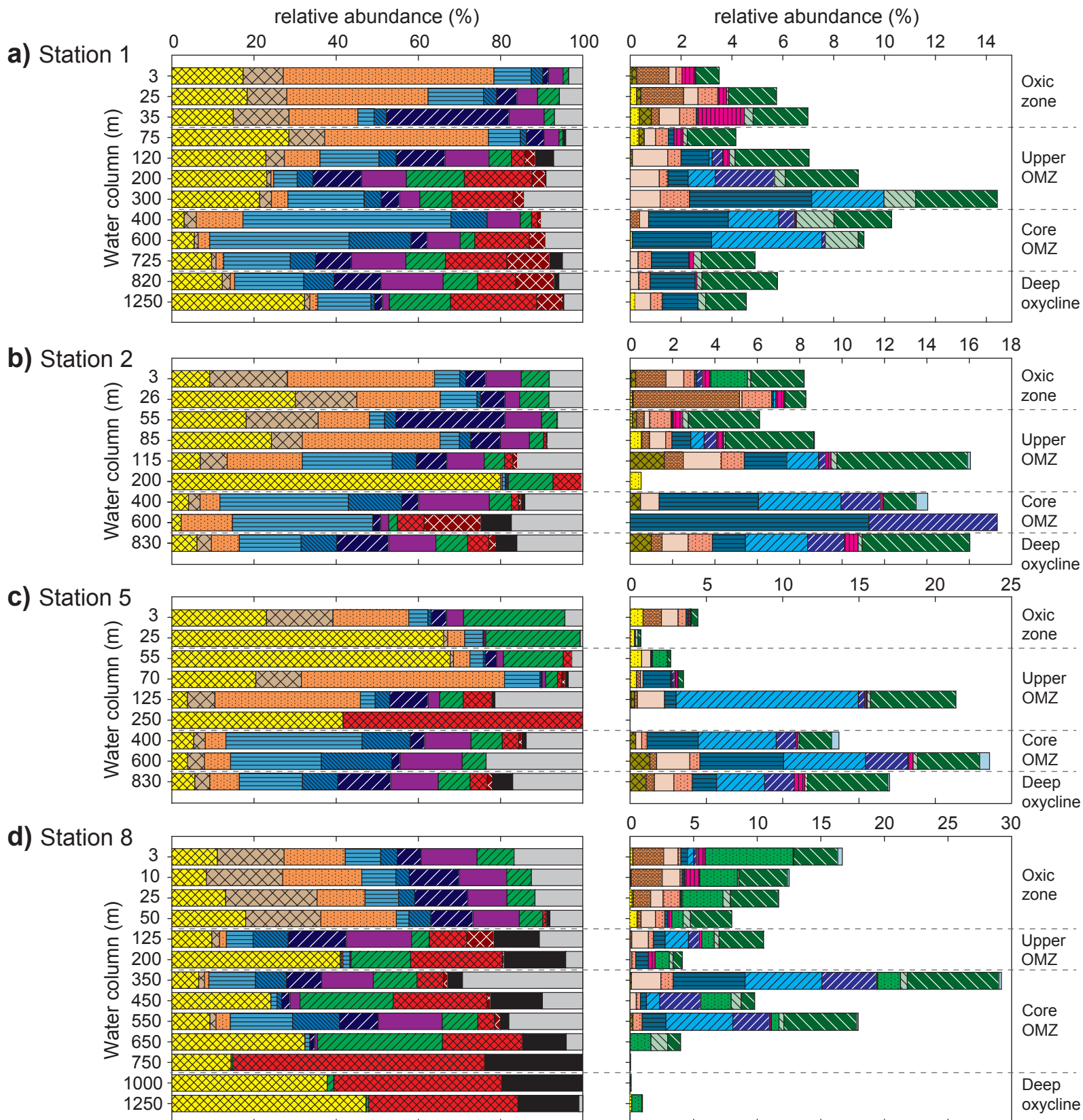
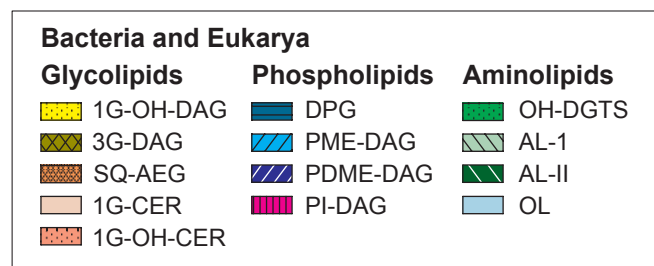
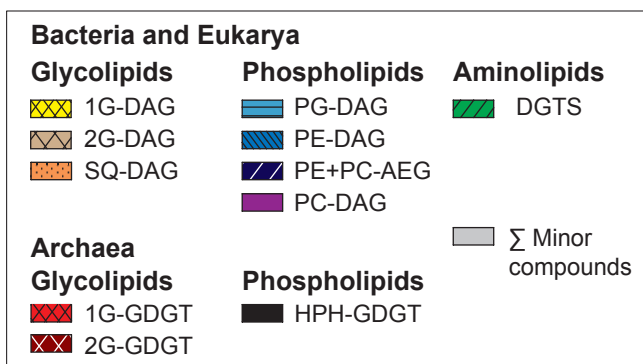


fig05

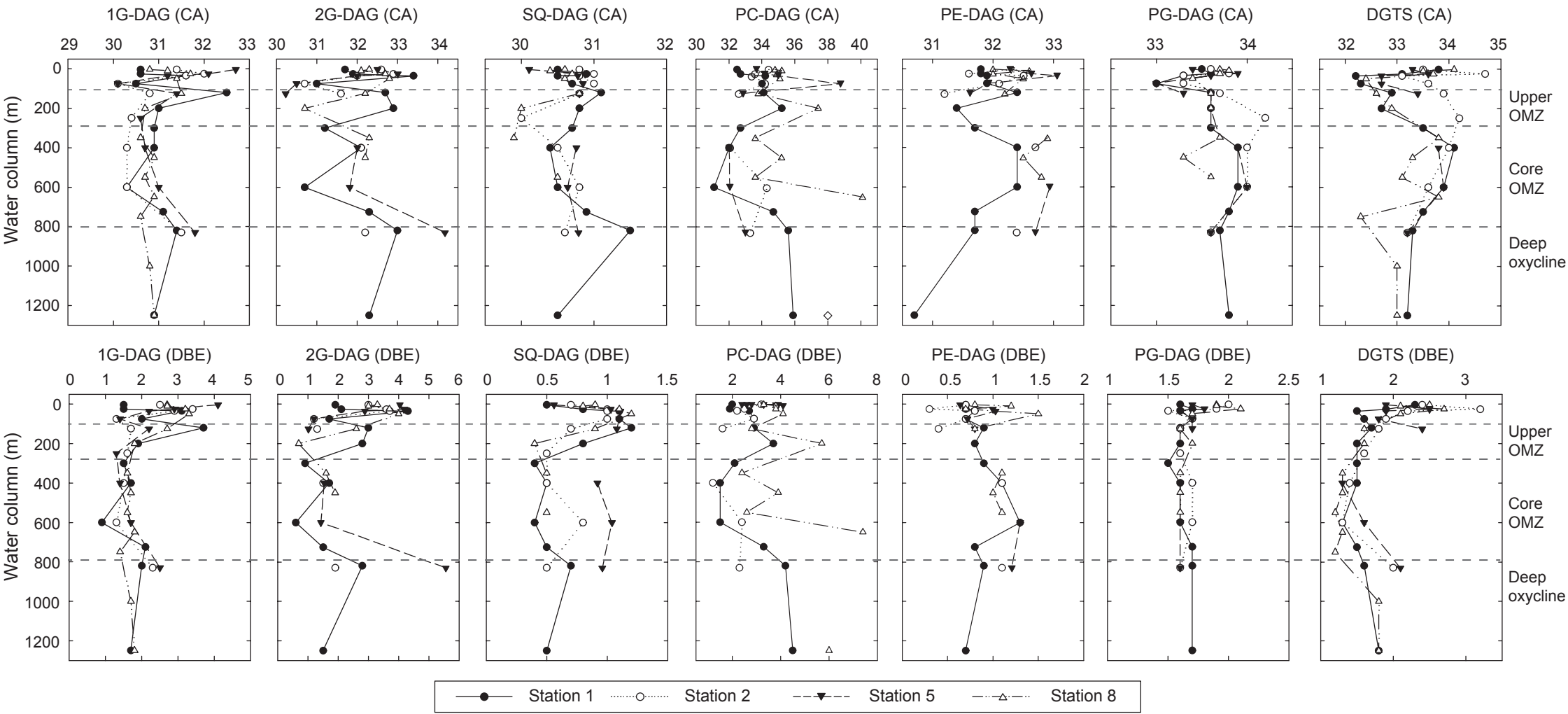
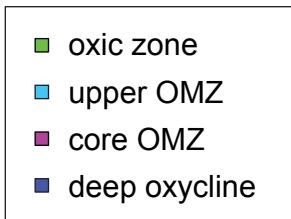


fig06



(p < 0.001)	r ²	(p < 0.001)	r ²
Oxygen	0.54	POC	0.40
Phosphate	0.48	Depth	0.39
Fluorescence	0.46	Nitrate	0.38
TN	0.43	Chl a	0.28

